



VCU

Virginia Commonwealth University
VCU Scholars Compass

Theses and Dissertations

Graduate School

2017

PNPase IN C. ELEGANS: MUTAGENIC ANALYSIS TO COMPLEMENT KNOCKDOWN STUDIES

Danielle K. Seibert
Virginia Commonwealth University

Follow this and additional works at: <https://scholarscompass.vcu.edu/etd>



Part of the [Genetics Commons](#), and the [Molecular Genetics Commons](#)

© The Author

Downloaded from

<https://scholarscompass.vcu.edu/etd/5040>

This Thesis is brought to you for free and open access by the Graduate School at VCU Scholars Compass. It has been accepted for inclusion in Theses and Dissertations by an authorized administrator of VCU Scholars Compass. For more information, please contact libcompass@vcu.edu.

PNPase IN *C. ELEGANS*: MUTAGENIC ANALYSIS TO COMPLEMENT KNOCKDOWN
STUDIES

A thesis submitted in partial fulfillment of the requirements for the degree of Master
of Science at Virginia Commonwealth University

By DANIELLE SEIBERT

Bachelor of Science, LIMESTONE COLLEGE 2012

Director: RITA SHIANG, Ph.D.

ASSOCIATE PROFESSOR

DEPARTMENT OF HUMAN AND MOLECULAR GENETICS

Virginia Commonwealth University

Richmond, Virginia

July 2017

ACKNOWLEDGEMENTS

First and foremost, I would like to thank my PI and mentor Dr. Rita Shiang. Her extensive personal and professional guidance is greatly appreciated and has taught me much about scientific research as well as life and Lindy Hop in general.

Secondly, I would like to thank my committee members Dr. James Lister and Dr. Jill Bettinger for their guidance in all aspects of this project. A special thanks to Dr. Bettinger for her expertise on the *C. elegans* model organism system, really expensive microscopes, and laboratory fire safety standards. Additional thanks to Dr. Lister, for the use of his carpeted lab floor, in order to better approach a more holistic method of procrastination following late nights in the ER.

I would also like to thank Dr. Laura Mathies for her added expertise on the *C. elegans* model system. Her insight and advice were crucial accompanied by her steady hands for all animal injections.

Further thanks to all past and present Shiang lab members. Without them my experience here would have been of a more dismal sort.

Lastly, a great deal of thanks and appreciation goes to all of the continued support from my close friends and family, most importantly of which is my mother. Without her relentless and unwavering encouragement, along with daily positive affirmations, I would not have come as far as I have. I love you mostest.

If this thesis is not a success, I dedicate it to the kid who totaled my car, along with the burglars who later, broke into my new vehicle, raided my glove compartment, and stole a GPS, 2 pairs of sunglasses, and my Tic-tac's. Also to the influenza virus, which presented itself somewhere around 1/3 of the way through the fourth chapter.

Table of Contents

| | Page |
|---|------|
| Acknowledgements..... | ii |
| List of Tables and Figures..... | vi |
| List of Abbreviations..... | ix |
| Abstract..... | xi |
| Clarification of Contributions..... | 2 |
| CHAPTER | |
| 1. PNPASE INTRODUCTION..... | 3 |
| a. PNPT-1..... | 3 |
| b. PNPase Structure..... | 4 |
| c. PNPase Localization..... | 7 |
| d. Mitochondria..... | 7 |
| e. Reactive Oxygen Species..... | 10 |
| f. PNPase in Mitochondria..... | 11 |
| g. Functional Studies of PNPase..... | 14 |
| i. Studies in Bacteria..... | 14 |
| ii. Knockdown and Knockout Studies..... | 17 |
| ii. Overexpression Studies | 18 |
| h. Human Diseases | 20 |

| | |
|---|----|
| i. <i>C. elegans</i> | 22 |
| j. PNPase in <i>C. elegans</i> | 26 |
| k. Longevity Pathways | 27 |
| 2. MATERIALS AND METHODS | 32 |
| a. <i>C. elegans</i> culture and maintenance..... | 35 |
| b. Bleaching of adult <i>C. elegans</i> | 35 |
| c. Extracting RNA from <i>C. elegans</i> | 35 |
| d. Generating cDNA from <i>C. elegans</i> | 36 |
| e. PCR | 37 |
| f. qPCR | 38 |
| g. Lifespan assays | 38 |
| h. PQ and NAC lifespan assays | 39 |
| i. ROS assay | 40 |
| j. Imaging of mitochondria..... | 41 |
| 3. RESULTS | 44 |
| a. Generation of PNPase mutant strains in <i>C. elegans</i> | 44 |
| c. Characterization of Lifespan of PNPase knockout in <i>C. elegans</i> | 46 |
| d. Confirmation of PNPase lifespan extension via increased ROS..... | 50 |
| e. Quantification of ROS in <i>pnpt-1</i> knockout..... | 58 |
| f. PNPase knockout and mitochondrial structure..... | 60 |

| | |
|--|----|
| g. PNPase knockout and <i>fzo-1</i> expression..... | 63 |
| h. Reconfirming <i>pnpt-1</i> mutations..... | 65 |
| 4. DISCUSSION | 67 |
| a. PNPase knockout in <i>C. elegans</i> increases lifespan | 68 |
| b. PNPase knockout and ROS production..... | 70 |
| c. PNPase knockout and effects on mitochondrial morphology..... | 72 |
| f. Conclusions | 74 |
| 5. APPENDIX: prior work in <i>C. elegans</i> | 75 |
| Literature Cited | 92 |

List of Tables and Figures

| | Page |
|---|------|
| Figure 1: Structure of PNPase..... | 6 |
| Figure 2: PNPase roles in subcellular localization..... | 13 |
| Figure 3: Lifecycle of <i>C. elegans</i> | 25 |
| Figure 4: <i>C. elegans</i> known longevity pathways..... | 28 |
| Figure 5: Heritable targeted gene disruptions in <i>C. elegans</i> using CRISPR | 34 |
| Table 1: PNPase Primer sequences and uses | 37 |
| Figure 6: PNPase deletion strains..... | 45 |
| Figure 7: PNPase knockout extends lifespan in <i>C. elegans</i> | 48 |
| Table 2: Mean lifespans and p-values for trials A-C as seen in Figure 7..... | 48 |
| Figure 8: Separate analysis of extended lifespan observed in Figure 7..... | 49 |
| Table 3: Mean lifespans and p-values for trials B-C as seen in Figure 8..... | 49 |
| Figure 9: N2 lifespan analysis on PQ and NAC..... | 52 |
| Table 4: Mean lifespans and p-values for trials A-C as seen in Figure 9..... | 53 |
| Figure 10: Cas9 1-2 lifespan analysis on PQ and NAC..... | 54 |
| Table 5: Mean lifespans and p-values for trials A-C as seen in Figure 10..... | 55 |
| Figure 11: Cas9 1-9 lifespan analysis on PQ and NAC..... | 56 |
| Table 6: Mean lifespans and p-values for trials A-C as seen in Figure 11..... | 57 |

| | |
|---|----|
| Figure 12: PNPase knockout does not increase ROS production..... | 59 |
| Figure 13: Mitochondrial cross-sectioning of an N2 animal..... | 61 |
| Figure 14: PNPase knockout does not affect mitochondrial size..... | 62 |
| Figure 15: PNPase knockout and <i>fzo-1</i> expression..... | 64 |
| Figure 16: Repeated genome sequencing of PNPase knockout animals..... | 66 |
| Figure 19: Verification of wCISD knockdown..... | 90 |

List of Abbreviations

AMP – ampicillin

Apaf-1 – apoptotic protease activating factor 1

ATP – adenosine triphosphate

Carb – Carbenicillin

clk-1 – clock abnormal protein 1

C. elegans – *Caenorhabditis elegans*

Cas 9 – CRISPR associated protein 9

CISD - CDGSH Iron-Sulfur Domain-Containing Protein

CRISPR – clustered regularly interspaced short palindromic repeats

DEPC – diethylpyrocarbonate

DIC – differential interference contrast

DIDMOAD – diabetes insipidus, diabetes mellitus, optic atrophy, and deafness

DNA – deoxyribonucleic acid

Drp1 – dynamin-related protein 1

dsDNA – double stranded DNA

dsRNA – double stranded RNA

ER – endoplasmic reticulum

ERIS – endoplasmic reticulum intermembrane small protein

ETC – electron transport chain

IFN – interferon

IGF-1 – insulin growth factor 1

IPTG – isopropyl β -D-1-thiogalactopyranoside

isp-1 – iron sulfur protein 1

LB – Luria broth

Mfn1 – mitochondrial fusion protein 1

Mfn2 – mitochondrial fusion protein 2

M-MLV – Maloney-murine leukemia virus

MMP1 – metal metallic protease 1

mRNA – messenger RNA

MTS – mitochondrial targeting sequence

NAC – n-acetyl cysteine

NGM – normal growth medium

Opa1 – optic atrophy 1

OXPPOS – oxidative phosphorylation

PCR – polymerase chain reaction

PNPase - Polyribonucleotide phosphorylase

PNPT-1 - polyribonucleotide nucleotidyltransferase 1

PQ – paraquat

RBD – RNA binding domain

RISC – RNA-induced silencing complex

rRNA – ribosomal RNA

RNA – ribonucleic acid

RNAi – RNA interference

ROS - Reactive Oxygen Species

RPH – Rnase PH

siRNA – small interfering RNA

SOD2 – superoxide dismutase 2

tRNA – transfer RNA

TEM – transmission electron microscope

WLB – worm lysis buffer

WS1 – Wolfram Syndrome 1

WT – wild type

ABSTRACT**PNPase IN *C. ELEGANS*: MUTAGENIC ANALYSIS TO COMPLEMENT KNOCKDOWN STUDIES**

By Danielle Seibert, B.S.

A thesis submitted in partial fulfillment of the requirements for the degree of Master of Science at Virginia Commonwealth University

Virginia Commonwealth University, 2017

Major Director: Rita Shiang Associate Professor, Department of Human and Molecular Genetics

PNPase is a gene implicated as a potential target for cancer therapy; human mutations also present with deafness, myopathies, and neuropathies. In this study, *C. elegans* was used to investigate the effect of knocking out PNPase in a whole animal. *C. elegans* knockdown studies have reported an extended lifespan via an increase in ROS production. Further noted are larger mitochondria and an increase in *fzo-1* expression. Knockout animals previously constructed using CRISPR/Cas9 were used for this study. We aimed to confirm these findings validating previous studies. It was discovered that PNPase knockout animals demonstrated a similar lifespan extension that was resolved with the addition of antioxidants in the media. All subsequent findings contradicted those of the knockdown studies. Resequencing of knockout animals demonstrated no existing mutation and studies were discontinued. New mutants will advance future analyses and validate prior investigations.

Clarification of Contributions:

I have been privileged to have the help of many people throughout the course of my thesis work. Substantial contributions are here represented as Chapters II, III, and IV, and are detailed below. All work except that described below and cited in the text was exclusively my own.

The CRISPR / Cas9 knockout animals (1-2, 1-6, 1-9) were generated by Dr. Laura Mathies and Laura Lambert. Laura Lambert created the clones containing the guide RNAs and Dr. Mathies performed injections on N2 and CF3152 animals for both studies discussed here. Laura Lambert developed the Ex3 RNAi knockdown construct. Laura Lambert carried out subsequent knockdown studies. I supplemented her work with additional attempts to validate PNPase knockdown via western blot. Mitochondrial images were obtained by Judy Williamson of VCU's microscopy core. Dr. Rita Shiang helped attain final sequencing results on the predicted knockout animal lines.

CHAPTER 1: PNPase INTRODUCTION

I. PNPT1:

PNPT1 is a, highly conserved, nuclear encoded gene that produces a 3'-5' exoribonuclease. This member of the polynucleotide phosphorylase family localizes to the inner membrane space of the mitochondria as well as the cytosol (Piwowarski et al, 2003; Chen et al, 2006; Leszczyniecka et al, 2002; Sarkar and Fisher, 2006). PNPT1 is found on chromosome 2p15-2p16.1 in humans, spans 60 Kb, and contains 28 exons (Leszczyniecka et. al., 2003). *hPNPase^{old-35}* (human PNPase) was first discovered as an upregulated gene in an overlapping pathway screen intended to identify genes that were differentially regulated in senescent progeroid fibroblasts and terminally differentiated HO-1 human melanoma cells (Leszczyniecka et al., 2002). The screen identified a total of 75 genes designated old-1 through old-75. Old-35 was subsequently identified as showing significant homology to PNPase from other species, and thus labeled as human PNPase, or *hPNPase^{old-35}* (Leszczyniecka et. al., 2002). This multi-functional enzyme has been shown to have a role in specifically degrading c-myc mRNA (Sarkar et al., 2003; Sarkar et. al., 2005), miR-221, miR-222, and miR-106b (Das et. al., 2010). The exoribonuclease was also found to aid in regulating translocation of small RNAs into the mitochondria, such as MRP (mitochondrial RNA processing), 5S rRNA, and RNase P (Wang et al., 2010; Wang et

al., 2012). At the transcriptional level, PNPT-1 was found to have been induced by type I interferon (IFN- α and β). An IFN-stimulated response element (ISRE) was identified in the promoter of *hPNPase*^{*old-35*}; mutating this site was found to eliminate induction of gene expression by IFN (Leszczyniecka et al., 2003).

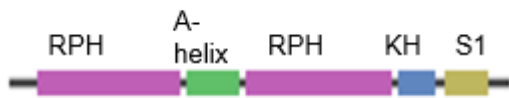
II. PNPase Structure

PNPase is an evolutionarily conserved protein. It is found in the majority of organisms including bacteria, plants, and humans with the exception of fungi, trypanosomes and the entire domain Archaea (Sarkar and Fisher, 2006). Human PNPase is known to have five conserved motifs: two RNase PH (RPH) domains at the amino terminal separated by an α -helix, unique to PNPase, and two C-terminal RNA binding domains (RBD) (KH and S1) (Figure 1A) (Symmons et al 2000; Leszczyniecka et al 2002; Raijmakers et al 2002; Symmons et al 2002; Leszczyniecka et al 2004). PNPase in *C. elegans* is similar, in that it has the two RPH domains and the two C-terminal RBD, but lacks the α -helix (Figure 1B). PNPase in plants contain an N-terminal chloroplast-transit peptide (cTP) or a mitochondrial-targeting sequence (MTS), while other organisms contain only the N-terminal MTS. Deletion studies in bacteria have shown that deletion of either the RBD, KH, or S1 domains will reduce

the ribonuclease activity of PNPase by 19-fold (KH) or 50-fold (S1). Deletion of both reduces activity to 1% (Stickney et al., 2005).

In humans, the protein PNPase is 783 amino acids long, with a weight of 86 kDa. In its primary location, the mitochondria, the protein assembles into a homotrimer or a dimer of two homotrimers (Piwowarski et. al., 2003; Rainey et. al., 2006). When attempting to determine the minimum active region, mutation analysis showed that both the RPH domains have equal enzymatic ribonuclease activity. It was found that the presence of either RPH domain is sufficient for complete enzymatic activity. Additionally, hPNPase maintains enzymatic activity when both RBDs have been deleted, thus indicating that the RPH domains may play a role in RNA binding in humans (Sarkar et. al., 2005).

A:



B:

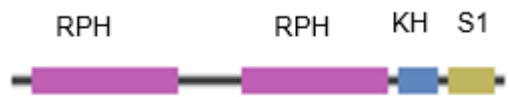


Figure 1: Structure of PNPase

The human protein (A) has 2 RNase PH (RPH) domains separated by an alpha helix, specific to PNPase, and followed by two RNA binding domains: KH and S1. The *C. elegans* structure of PNPase (B) contains the two RPH domains along with the two RNA binding domains; the intervening alpha helix is absent. (www.ncbi.nlm.nih.gov)

III. PNPase Localization

The MTS at the amino terminus of human PNPase localizes the exoribonuclease to the mitochondria (Piwowarski et. al., 2003). Subfractionation studies further localized PNPase to the inner membrane space of the mitochondria, more specifically as an inner membrane bound peripheral protein (Chen et. al., 2006). PNPase is imported to the inner membrane space via an i-AAA protease Yme-1 dependent mechanism (Rainey et. al., 2006). Additional studies have shown that *hPNPase^{old-35}* also localizes to the cytoplasm where it can help to degrade specific mRNA and miRNAs (Leszczyniecka et. al., 2002; Sarker et. al., 2003; Chen et. al., 2006; Das et. al., 2010).

IV. Mitochondria

The mitochondria are the location of cellular respiration. This double-membraned organelle is the primary site for ATP synthesis that takes place via a series of respiratory complexes known as the electron transport chain (ETC). The mitochondrial genome is made up of double stranded DNA that is inherited through the female oocyte, and thus solely through the maternal lineage. It is approximately 16 Kb in length and circular in nature. Unlike nuclear DNA, the mitochondrial genome

only contains 37 genes. Because of the size of its genome, the mitochondria are not able to independently produce the many proteins it needs for complete functionality. It must therefore rely heavily on gene products imported from the nucleus. Mitochondrial genes, from both strands, are transcribed in a polycistronic manner. This means that the large mitochondrial mRNA products contain genomic information that codes for many different proteins. These are subsequently spliced into functional tRNA, rRNA, and mRNAs (Chial et. al. 2008).

Along with its role in energy metabolism, the mitochondria play an essential role in calcium signaling and cellular homeostasis. A defined level of calcium is necessary to maintain homeostasis within the cell. If calcium levels within the cell surpass that of the threshold capabilities, the mitochondrial membrane potential will collapse resulting in cellular apoptosis (Rizzuto et. al., 2009). Mitochondria have also been found to have a role in non-calcium induced apoptosis secondary to an altered membrane potential from other apoptotic pathways. When the membrane potential changes detrimentally the mitochondria release caspase activators that deactivate proteins that inhibit apoptosis along with cytochrome C, known to bind to Apaf-1 (apoptotic protease activating factor - 1) (Green, 1998; Fesik and Shi, 2001). Furthermore, the mitochondrion acts as a calcium reservoir, with calcium being taken up into the matrix for storage (Brighton and Hunt, 1974; Miller, 1998). The

mitochondria are not simply static organelles, but engage in fission and fusion as a response to cellular conditions; the rate of this is determined by the differing metabolic demands and is crucial to the overall health of the cell.

Fission is a necessary process that ensures faithful inheritance and adequate mitochondrial populations in daughter cells during cellular division. Drp1, a cytosolic dynamin family member, mediates this process by forming a spiral around the mitochondria, constricting, and severing through both membranes. Fission can also be used to sequester debris to one end of the organelle for disposal when mitochondria accumulate excessive damage. Subsequent division occurs and the mitochondria containing the damaged debris undergo autophagocytosis allowing the healthy organelle to continue performing its normal functions. (Youle and van der Bliek, 2012).

The act of fusion can also help to mitigate cellular stress by mixing the contents of partially damaged mitochondria as a form of complementation. Mammalian cells contain three GTPases in the outer membrane of the mitochondria. These transmembrane proteins, Mfn1, Mfn2, and Opa1, are all required for proper fusion (Martinou and Youle, 2011). As a triggered response to cellular stress, fusion can furthermore become enhanced under starvation conditions. Moreover, the process can be used to rescue mutations within the mitochondrial genome (Tondera et. al.,

2009; Gomes et. al., 2011; Rambold et. al., 2011).

X. Reactive Oxygen Species (ROS)

ROS such as hydrogen peroxide, the hydroxyl radical, and superoxide are generated under hypoxic conditions. Complex III of the ETC has the capability of circulating superoxides into the intermembrane space of the mitochondria; thus, a major source for ROS production is cellular respiration. While large increases in ROS can damage proteins, lipids, and DNA, smaller volumes have been shown to activate signaling pathways leading to proliferation and transcription (Trachootham et. al., 2008; Droge, 2002; Thannickal and Fanburg, 2000).

There is strong evidence to show ROS are upregulated in tumors and can lead to induction of signaling networks that cause tumorigenesis and metastasis (Weinberg and Chandel, 2009). A variety of mechanisms exists to counteract the effect of superoxides, namely superoxide dismutases (SODs). This family of dismutases is able to convert the superoxide into hydrogen peroxide, which can then be eliminated by a variety of other peroxidases and peroxiredoxins (Sena and Chandel, 2012). Recent studies have shown that a slight increase in ROS, rather than being harmful, will activate beneficial stress responses in animals extending their lifespan (Schulz et. al., 2007; Zarse et. al., 2012).

VI. PNPase in Mitochondria

Multiple studies have been previously performed to determine if *hPNPase^{old-35}* plays a role in mitochondrial homeostasis given its primary localization to the inner membrane space. Overexpression studies have indicated that *hPNPase^{old-35}* plays a role in ROS induction (Sarkar et. al., 2004; Sarkar and Fisher, 2006). An observable change in the mitochondria is found in knockdown and knockout experiments. Mitochondria were observed to become more filamentous and granular shaped in HEK293T knockdown cells. Furthermore, a decreased membrane potential was discovered along with a reduction in enzymatic activity of coupled respiratory complexes I / III, II / III, and the individual complexes IV and V. Auxiliary studies concluded that *hPNPase^{old-35}* knockdown reduces ATP levels and causes lactate accumulation (Chen et. al., 2006).

Additionally, *hPNPase^{old-35}* plays a role in importing small RNAs into the mitochondria, specifically RNase P RNA, MRP RNA, and 5S RNA. RNase P is a ribozyme known to cleave precursor sequences from tRNA molecules. MRP RNA is involved in the initiation of DNA replication in the mitochondria. 5S RNA is a small ribosomal RNA

molecule, a subunit that, during translation, contributes to the function of the large ribosome as a whole. *hPNPase^{old-35}* recognizes these RNAs via a specific stem-loop motif. It is important to note, the two roles PNPase plays are not dependent on one another: mutations affecting small RNA import do not affect the RNA processing role (Wang et. al., 2010; Wang et. al., 2011). Figure 2 summarizes the multiple roles PNPase plays in the cell, as well as its multiple locations it can be found.

VII. Functional Studies of PNPase

a. Studies in Bacteria

Bacterial PNPase is involved in a majority of the bacterial cell functions that are essential for growth, development, and survival. Studies in bacteria demonstrate PNPase has variable functionalities including, but not limited to, RNA decay and other posttranscriptional modifications of mRNA, which are essential for growth and survival (Deng et al. 2014; Regonesi et al. 2006). A gene knockout study in *Yersinia pestis* determined PNPase increases the degradation of Hfq-free structured RNA; the study involved both single and double (*hfq* / *hfq-rnc*) mutants. In bacteria, the RNA chaperone Hfq is thought to aid in guiding sRNAs (small RNAs) to their mRNA targets while stabilizing them from degradation by RNase E (Deng et al. 2014). Small RNAs are RNA molecules that are usually less than 200 bp in length and are not translated into proteins. PNPase and RNase E are two of the major components of RNA degradation and are subsequently recruited for cleavage by the Hfq chaperone. Knockout studies involving RNase G, RNase II, and RNase III deletions, showed similar results to those involving Hfq-mutations (Deng et al. 2014). The *pnp* gene was found to be upregulated in studies using double (*hfq-rnc*) and triple (*hfq-rnc-rnb*) mutants as compared to single *hfq* mutants. Additional experiments noted a decrease in sRNA transcripts when PNPase was upregulated. This confirmed the idea that PNPase is the primary exoribonuclease responsible for sRNA degradation in an *hfq* free

environment (Deng et al. 2). Similarly, a gene knockout study in *Escherichia Coli* investigated the involvement of PNPase in RNA binding and degradation. Findings showed an impairment of these processes in G454D PNPase mutants (Regonesi et al. 2006). The Glycine at position 454 was found to be essential for the structural integrity of the enzyme multimer and overall stability of the degradosome.

PNPase mediates different posttranscriptional roles in bacteria. In pathogenic bacteria, a large number of sRNAs modulate response to stress, adaptation, and the production of virulence factors (Andrade and Arraiano 546; Haddad et al. 6; Viegas et al. 7656). PNPase is essential in the generation of outer membrane proteins important for bacterial motility. One in particular, the outer membrane A gene (*OMP A*), is involved in the pathogenic initiation in bacteria aided by motility. The small noncoding RNAs *micA* and *RybB* are stationary phase regulators involved in the synthesis of outer membrane proteins. *RybB* is crucial in the regulation of outer membrane proteins B and C, while *micA* regulates outer membrane A protein. Because of the posited involvement of PNPase in the generation of the small noncoding RNAs *micA* and *RybB*, significant decreases in the products regulated by these RNAs confirms the involvement of the enzyme in the regulatory process (Andrade and Arraiano et al.). Decreased *ompA* quantities have been correlated with reduced *micA* levels, which are modulated by PNPase enzyme systems. Furthermore,

ompA levels and *micA* RNA concentrations have been found significantly reduced in *E. coli* bacteria containing *pnp* mutations (Andrade and Arraiano et al.). Additionally, studies in *Campylobacter jejuni* have demonstrated a reduced bacterial motility in *pnp* mutant species, which was later reversed by complementation with wild-type *pnp* animals (Haddad et al. 2012).

PNPase is further implicated in bacterial adaptability, along with survival and growth. Additional studies in *C. jejuni* have shown that bacteria require PNPase for adhesion and invasion of host cells, and bacterial colonization (Haddad et al. 2012). Similar findings were made following studies performed with *E. coli*, (Andrade and Arraiano 544; Favaro and Deho 5280-5281), and studies that utilized the *Salmonella* species (Viegas et al. 7656; Adolaib 79). Studies in *Salmonella* demonstrated many sRNAs are induced when under specific stress conditions; these include DNA damage, cold shock, osmotic stress, iron stress, and oxidative stress (Viegas et al. 2007). Wild-type *Salmonella* species express virulence genes, for pathogenic entry, and concomitant increments, in CsrB and CsrC protein subunits throughout the early stationary phase. Meanwhile the virulence factors for host survival were expressed in the middle and late phases. Furthermore, PNPase was found to have a profound effect on the stability of MicA, CsrB, CsrC, and SraL. These sRNAs were found upregulated in the absence of PNPase via northern blot analysis. PNPase was also

found to be a key regulator in the decay of all 4 sRNAs studied. These findings demonstrate the underlying involvement of PNPase in RNA decay and the posttranscriptional production of sRNAs. PNPase enzyme is necessary for the formation of the regulatory sRNAs, which, together with RNA-binding proteins carbon storage regulator A (CsrA) form a complex that enables the *Salmonella* species to produce adapt to its environment and survive. The CsrB and CsrC produced in the stationary phase of the bacterial growth phase are indications of the multivariate cellular effects of PNPase on bacteria (Viegas et al. 2007). Similarly, the adhesion and invasion molecules, as well as those involved in the comparative colonization of the host cells are bacterial adaptation and survival factors (Haddad et al.). Their elevated expression during stress (stationary phase) reflects PNPase involvement in the adaptability by redirecting the generation of sRNAs and protein regulators to enable the bacteria survive in otherwise adverse environments. The decreased adaptability and survival, as evidenced by the reduced molecules (*Lux S*, *peb3*, *katA*, and *hsp90*) in *pnp* mutant types confirm PNPase involvement in the formation of virulence factors.

b. Knockout and Knockdown Studies

In vivo studies have indicated that total knockout of *Pnpt1* in mice is embryonic lethal, thus showing its importance in development. Further studies report targeted liver knockout results in a decrease in the activity of the respiratory chain as well as

causing disordered, circular, and smooth mitochondrial cristae (Wang et al., 2010). Additionally, PNPase knockdown in a melanoma cell line HO-1 results in filamentous and granular mitochondria, a decrease in membrane potential, and a decrease in the enzymatic activity of the respiratory complexes (Chen et al., 2006).

c. Overexpression Studies

Overexpression studies with *hPNPase*^{old-35} in HO-1 cells were performed in order to investigate the mechanism of growth inhibition. Two unique methods were used: slow and sustained overexpression via a low multiplicity adenoviral vector and rapid overexpression via a high multiplicity adenoviral vector. The results demonstrated different phenotypes for each method of overexpression. Slow and sustained overexpression, initiated to determine the mechanism behind inhibition of colony formation seen in HO-1 cells, resulted in growth inhibition and induction of a senescent-like phenotype, which ultimately resulted in apoptosis. Analysis of the cell cycle of these cells indicated that there was an initial G1/S or G2/M arrest followed by apoptosis (Sarkar et. al., 2003; Sarkar et. al., 2005; Van Maerken et al., 2009). Conversely, rapid overexpression, used to further investigate the mechanism behind PNPase overexpression induced growth arrest and promoted apoptosis without any accompanying cell-cycle changes (Sarkar et al., 2003).

Furthermore, slow and sustained overexpression downregulated c-myc mRNA and protein, a key mediator in the G1/S transition. It was shown that c-myc overexpression would protect against cell death caused by overexpression of *hPNPase^{old-35}* (Sarkar et. al., 2003). It is thought that *hPNPase^{old-35}* specifically recognizes c-myc mRNA via the 3' UTR, as c-myc mRNA with no 3'UTR was resistant to degradation by *hPNPase^{old-35}* (Sarkar et. al., 2003; Sarkar et. al., 2006). As no RNA-binding site has been identified in PNPase from any species, it is thought that secondary structure of the RNA may be the determining factor in RNA specificity (Sohki et. al., 2013). Not only is c-myc specifically degraded, but it has also been found that *hPNPase^{old-35}* overexpression also degrades certain mature miRNA species such as miR-221, miR-222, and miR-106b (Das et. al., 2010). miR-221 is frequently overexpressed in a variety of human cancers, targeting a large set (602) of genes involved in oncogenic pathways (Lupini et. al., 2013). miR-222 is additionally found to be upregulated in a variety of cancers and has been found to target MMP1 (metallic protease 1) and SOD2 (superoxide dismutase 2) (Liu et. al., 2009). Lastly, miR-106b has been found to target a number of tumor suppressor genes (Liu et. al., 2014). Given the roles these miRNAs play in cancer progression, elevated *hPNPase^{old-35}* may prove to be an attractive anti-cancer target.

VIII. Human Diseases

More recently, a PNPase mutation has been found in individuals with hereditary hearing loss (von Ameln et. al., 2012). A second mutation was identified in a family with myopathy, encephalopathy, and neuropathy (Vedrenne et. al., 2012). Both expressed hallmark characteristics of classic mitochondrial disorders. The findings demonstrate how important PNPase is in mitochondrial function, cellular senescence, and terminal differentiation throughout development. Subsequently, these conclusions validate the multiple functional roles PNPase plays within the cell.

Investigation into one family (family A) revealed a PNPase mutation that resulted in a significant decrease of the 5S rRNA import. The affected individuals were also found to have a reduced amount of mature MRP-RNA in the mitochondria, but mtDNA levels were within normal limits. The observations, noted in family A, demonstrate the importance of the role of PNPase in small RNA import and, if disrupted, the detrimental effects it can have on an organism (Vedrenne et. al., 2012).

Another family (family B) possessed a different PNPase mutation. Unlike the first, this mutation manifested itself as hereditary hearing loss. On further studies, affected individuals in family B were found to have a decreased amount of RNase P imported into the mitochondria. Within these individuals, PNPase was not able to properly homotrimerize and the mutation behaved as a hypomorph.

Family B displayed a less severe phenotype as compared to family A. It was hypothesized that the hypomorphic form of PNPase led to the decrease in small RNA import, which subsequently affected the tissue of the inner ear, but not the outer ear. It was further postulated that this was because the inner ear specifically requires a greater amount of energy for proper development. It was also thought that a variety of phenotypic variation would be found in families with differing severities of mutations, and thus functional deficits, of PNPase (von Ameln et. al., 2012).

hPNPase is involved in global cellular functions including cell communication, chromosomal organization, and cell cycle progression among others (Sokhi et al. 2014). HO-1 and HeLa studies have further shown the global effects of hPNPase on cellular homeostasis. For example, hPNPase overexpression in HeLa cells exposed to oxidative stress (excess hydrogen peroxide) increases cell viability and reduces RNA oxidation, while hPNPase knock out leads to increased oxidative stress-induced RNA damage and eventual cell death (Wu and Zhongwei 290). PNPase has been shown to bind oxidized RNA (8-oxoG oligonucleotides) thereby facilitating their sequestrations, aiding in its removal and conferring quality to RNA, of which mutated *pnpt* products cannot. Rare variants found in *PNPT1* have shown significant RNA dysregulations that predispose to neurodegenerative and neurological disorders like hearing loss. These variants cause oxidative phosphorylation damage evidenced in

hearing loss. The phenotypic manifestations of this damage include severe axonal neuropathy, auditory neuropathy, intellectual disabilities, optic atrophy, and chronic respiratory and gut disturbances (Alodaib et al., 2017).

The number of mitochondria per cell varies depending on the type of cell and tissue along with the specific energy needs. For example, a cardiac muscle cell would contain significantly more mitochondria than a lymphocyte, while mature red blood cells have no mitochondria. Each mitochondrion contains its own circular genome, which is similar in structure to that of bacteria. Mitochondrial disorders often present with a wide variety of clinical and phenotypic symptoms due to the variable number of mitochondria per cell.

VIII. *C. elegans*

Caenorhabditis elegans is a free-living soil nematode that is frequently used as a model organism for a variety of human diseases and processes. The adult worm is approximately 1 mm long with 959 somatic cells, and is easily grown, on a bacterial lawn, in a lab environment. These animals exist mainly as hermaphrodites (XX), though there is a less common male adult (XO) form. Their attractiveness as a model organism exists in their short three-day life cycle (Figure 3) and life span (at 20°C) of

approximately three weeks. Furthermore, these animals are ideal candidates for study given their fully sequenced and conserved genome, ease of growth, small size, and completely mapped cell lineage. Of note, *C. elegans* remain transparent throughout their entire life cycle, enabling cell-level examination via differential interference contrast (DIC) microscopy (Corsi et. al. 2007). Though anatomically simple, *C. elegans* can be used to study many complex behaviors such as locomotion, foraging, feeding, defecation, egg laying, sensory responses, mating, social behavior, and learning (Rankin, 2002; de Bono, 2003).

C. elegans are known to have neurons, gut, and muscles, along with other tissues that are similar in form, function, and genetics to those of human tissues. Because of this, these soil nematodes make an ideal organism for studying developmental and fundamental mechanisms that are underlying in human disease. This is of the utmost importance as many genetic experiments are unethical or otherwise impossible in higher-level organisms. Relevant disease studies include, but are not limited to, cancer, diabetes, neurodegeneration, muscular dystrophies, and aging (Lundquist et. al., 2004)

While there are significant benefits to using *C. elegans* as a model organism there are also select drawbacks. They are not ideal for studying the effects of manipulation on specific tissues. This is in part because worms lack some specialized

tissues more commonly found in higher-level organisms, for example, a heart or liver (Van Raamsdonk and Hekimi, 2010).

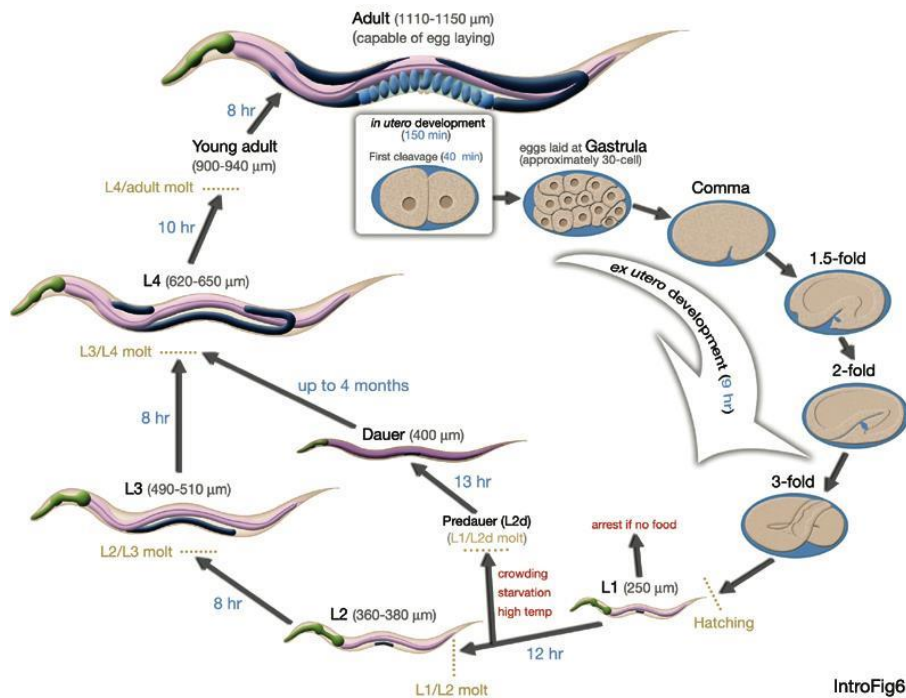


Figure 3: Lifecycle of *C. elegans*.

The lifecycle, including the size and time spent in each larval stage. Generally, early development to adulthood takes about 3 days. Eggs mature into the first larval stage, L1, approximately 10 hours after being formed. If sufficient food is available, the L1 animal will proceed into 3 further larval stages: L2, L3, and L4. After the L4 molt, the young adult will begin to form oocytes. If sufficient food is not present, the L1 larvae will proceed into a dauer stage, in which they can survive for anywhere between four to eight times their average life span. (www.wormatlas.org; Introduction to *C. elegans* Anatomy)

XIII. PNPase in *C. elegans*

This versatile model organism was used for further study of PNPase. The worm homolog of *pnpt-1*, BE0003N10.0, consists of 10 exons located on chromosome three. The transcript was originally identified during an RNAi profiling of embryogenesis. The screen aimed to identify all genes that were required for initial cellular division in the *C. elegans* embryo, thus demonstrating the importance of PNPase in development (Sonnichsen et. al., 2005). A deletion mutant (tm1909) was characterized by another group; their findings include phenotypes such as lethality and sterility. However, the *pnpt-1* mutation present in the tm1909 line affects more than just the *pnpt-1* gene. An upstream gene, *chin-1*, is also partially deleted. Thus, the gene responsible for the reported phenotypes cannot be differentiated, and is therefore unknown. *C. elegans* is a particularly attractive model to study gene function due to the ease of knocking down gene expression via RNAi. Given previous embryonic lethal results in mice with total knockout, a knockdown, would allow for a low level of expression and potentially avoid the lethality seen in other organisms. Pilot studies knocking down PNPase in *C. elegans* identified longevity as an initially identified phenotype. Additional studies from this lab confirmed the lifespan extension and reported an increase in ROS production among knockdown animals. Studies further found an increase in the size of knockdown animal mitochondria

along with an increase in fusion protein *fzo-1*. These are all preliminary studies performed in knockdown animals and need to be confirmed (Lambert, 2015).

X. Longevity Pathways

Worms have been used in a number of aging studies, which found that genes or interventions that extend the worm lifespan translate to other organisms, and vice-versa (Van Raamsdonk and Hekimi, 2010). There are a number of known pathways, that when disrupted, have demonstrated longevity in *C. elegans* (Figure 4):

- Disruption of mitochondrial function (Yang and Hekimi, 2010)
- Disruption of translation (Tacutu et. al., 2012)
- Disruption of insulin signaling (Schaffitzel and Hertweck, 2006)
- Caloric restriction (Schaffitzel and Hertweck, 2006)
- Exposure to xenobiotics (Shore, 2012)

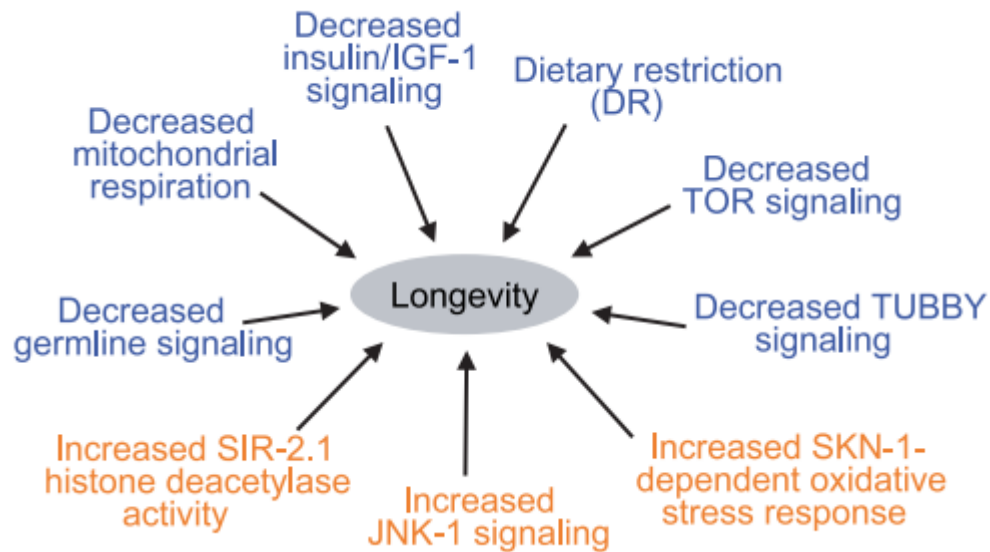


Figure 4: *C. elegans* longevity pathways.

Blue denotes a decrease in activity while orange indicates an increase in activity of the pathway/process leading to longevity (Schaffitzel and Hertweck, 2006). One of the best-characterized networks influencing aging is the effect on insulin signaling, specifically the insulin growth factor 1 (IGF-1) system/signaling. Inhibition of this pathway causes a constitutive dauer formation (see Figure 3), leading to lifespan extension in adult animals. Animals containing mutations in the IGF-1 pathway show increased fat storage, defective egg-laying, and high tolerance to a variety of stressors (Schaffitzel and Hertweck, 2006; Kenyon, 2005; Kenyon et. al., 1993; Kimura et. al., 1997; Paradis and Ruvkun, 1998).

One known mechanism for lifespan increase is ROS detoxification. The mitochondria are the major source of ROS in the cell, and as such, play a role in the length of the lifespan in *C. elegans* (Schaffitzel and Hertweck, 2006). Another study found that RNAi targeting of electron transport chain (ETC) complexes during larval development lead to a reduction in oxygen consumption and ATP levels. This also led to an observable lifespan extension (Dillin et. al., 2002; Lee et. al., 2003). Slight increases in ROS have similarly been found to increase lifespan (Yang and Hekimi, 2010).

An alternative mechanism for lifespan extension is caloric restriction. This mechanism, however, is not specific to *C. elegans*; the lifespan of yeast, flies, and rodents have been found to have up to a 50% extension with calorie reduction (Schaffitzel and Hertweck, 2006). The specific mechanisms behind this extension are yet to be fully understood. It is hypothesized that caloric restriction reduces the metabolic rate, and/or that it reduces the insulin/IGF-1 signaling (Bordone and Guarente, 2005; Walker et. al., 2005).

As a worm ages, a variety of physiological changes occur. These changes include, but are not limited to, a decrease in pharyngeal pumping, a decrease in movement, cessation of reproduction, and muscle wasting (Collins et. al., 2008). These same changes are observed in animals with extended lifespans. It is possible

that the observed physiological changes associated with aging are secondary to mitochondrial deterioration. It is well known that mitochondria play a crucial role in energy metabolism, however, it is not as well known that mitochondrial function progressively declines as an animal ages (Navarro and Boveris, 2007; Shigenaga et al., 1994). A number of *C. elegans* mutant lines have been created and established to study the effects of mitochondrial function on lifespan. Mutations in *mev-1* and *gas-1* have been shown to cause hypersensitivity to oxygen and superoxides subsequently shortening lifespans. Other animals with mutations in *clk-1*, *isp-1*, *lrs-2*, and *nuo-6* have been found to extend the lifespan of the animal. This is thought to be secondary to a decrease in oxygen consumption, a slight increase in ROS production, and a generalized slower growth pattern (Ishii et al., 1998; Kayser et al., 2001; Wong et al., 1995; Feng et al., 2001; Lee et al., 2003; Yang and Hekimi, 2010).

Given this lab's former findings in knockdown studies performed by Laura Lambert, it was of interest to repeat similar studies in knockout animals with the hopes of confirming these findings. It was previously found that *pnpt-1* knockdown animals demonstrated an increase in lifespan along with an increase in ROS. The noted increase in ROS was hypothesized to be a potential causative mechanism that led to the increased lifespan. Knockdown animals were further found to have an increase in *fzo-1* transcript production that potentially gives rise to observed

morphological changes and an increase in the overall size of the mitochondria. The knockdown animals were found to have a 67% decrease in mRNA and a 58% decrease in *pnpt-1* protein product. Given these findings, we would expect to find similar if not more severe results in knockout animals.

Chapter 2: Materials and Methods

Generation of *pnpt-1* mutant animals via CRISPR / Cas9

The new CRISPR/Cas 9 targeted genome editing system was used to create deletions in a targeted area of *pnpt-1*. A 20-nucleotide guide RNA sequence was cloned by Laura Lambert with the help of Dr. Laura Mathies. They used the Q5 site directed mutagenesis kit (NEB), with a 10ul reaction of PU6::unc-119_sgRNA vector (addgene). Peft-3::cas9-SV40-NLS::tbb-2 3'UTR (addgene) was used as the Cas9 vector with mCherry as a co-injection marker. A polymerase III promoter, which originated in a U6 locus drives transcription of the sgRNA. The sgRNA was comprised of a target sequence, which was designed by Laura Lambert, specific to a coding sequence in *pnpt-1*, and a scaffold sequence; both necessary for appropriate Cas9 binding. The SV40 NLS is a nuclear localization signal that was affixed to the 3' end of the Cas9 open reading frame in order to make certain the Cas9 nuclease is correctly directed to the nucleus. The cas9-SV40-NLS fusion protein was adjoined to an *eft-3* promoter sequence, which has shown a high level of effectiveness in germline expression. Non-homologous end joining (NHEJ) is the fundamental means of repair

for CRISPR/Cas9 guided double stranded DNA breaks (Friedland, 2013). This method of repair, however, may generate insertions and deletions (indels) to the affected sequence.

N2 wild type animals were microinjected with the vector expressing Cas9, the vector expressing the designed sgRNA, and mCherry. This fluorescent red co-injection marker, mCherry was used as a positive control for transformation in the F₁ progeny. Dr. Laura Mathies performed all injections into the gonad of N2 wildtype worms. Following initial injections, Laura Lambert picked P₀ animals onto NGM + OP50 plates and allowed them to recover overnight. F₁ progeny were isolated and observed; a small quantity of these animals was expected to be heterozygous for an indel. Laura Lambert screened F₂ animals. Laura Lambert individually isolated those that fluoresced red onto NGM + OP50 6 cm plates. She then allowed these animals to grow, developing potential knockout lines. Laura Lambert subsequently harvested an aliquot of these worms for DNA extraction and subsequent sequencing (Figure 5).

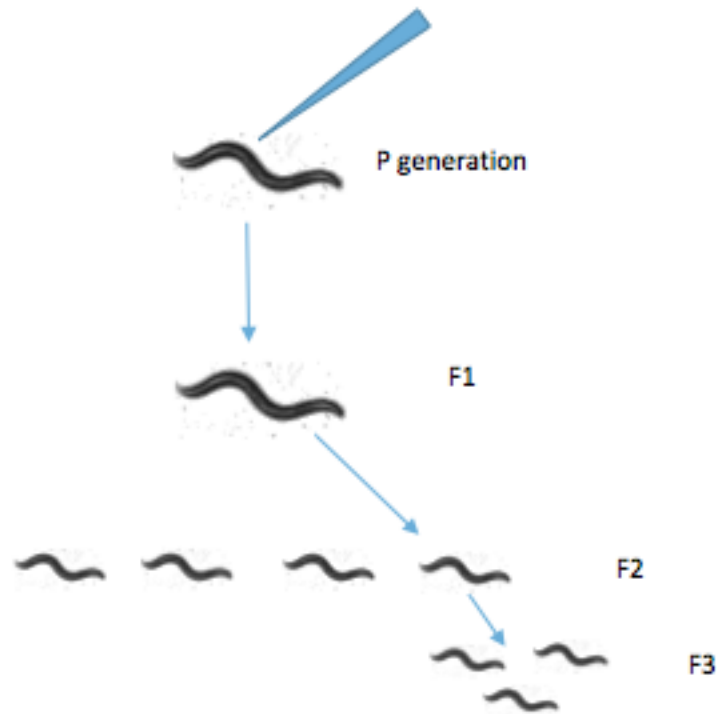


Figure 5: Heritable targeted gene disruptions in *C. elegans* using CRISPR

P generation: N2 animal's gonads were microinjected with 3 vectors as part of CRISPR / CAS9 site directed mutagenesis. The vectors encoded Cas9, sgRNA, and a vector driving expression of mCherry in body-wall muscles to label transformed F1 progeny. F1 progeny that fluoresced red were isolated. F2 animals that fluoresced were again isolated to develop animals with germline transmission. F3 progeny were picked to individual plates, grown, and genotyped.

***C. elegans* culture and maintenance**

C. elegans were grown on NGM plates seeded with 100 uL OP50 bacteria and maintained at 20°C. Worm plates were chunked every 3 days for strain maintenance and additionally, as needed, to prepare for experiments. All studies used N2 animals as wild type alongside CRISPR/CAS9 mutant lines 1-2, 1-6, and 1-9.

Bleaching of adult *C. elegans*

When plates of worms became contaminated with mold or bacteria, it was necessary to bleach the worms and transfer them to a new, clean plate. A bleach solution was made using 30% bleach with 0.6 N KOH and filter sterilized. On a fresh NGM + OP50 plate, a 20 uL aliquot of bleach solution was pipetted along the edge of the plate. Between 5 and 10 gravid, contaminated animals were picked and placed directly into the solution. The animal's cuticles are ruptured by the bleach solution allowing the eggs to be freed from within. The plates are subsequently incubated at 20°C face up, overnight. The following day, L1 larvae are transferred to a new plate.

RNA Extraction from *C. elegans*

Worms grown, on 15-20 6 cm plates, were washed off with 5 mLs M9 and gathered in a 15-mL conical tube. The worms were gently pelleted at 1000 rpm for 5 minutes, and the supernatant discarded. Worms were subsequently washed 3

additional times, in the same manner, using 5 mLs M9 for each wash. After the last of the supernatant was removed 200 uL Trizol reagent was added. Worms were then freeze-cracked by alternating 30s in liquid nitrogen and a 1-minute thaw at 37°C; this was repeated approximately 7 times. The Trizol/worm mixture was transferred to a 1.5 mL Eppendorf tube, 200uL chloroform added, and spun at 13,000 rpm, at 4°C, for 15 minutes. The clear fraction was transferred to a new 1.5mL tube, and an equal volume of 70% isopropanol was added. A Qiagen RNA prep kit was used to isolate RNA following the manufacturer's instructions as written. RNA that was not immediately used for subsequent experiments was stored at -80°C.

Generating cDNA from *C. elegans*

The following was added to a 0.7 mL tube: 1ug RNA, 100 ng oligo dT primer, 100 ng random primer, and DEPC H₂O to 12uL. The reaction was incubated at 70°C for 10 minutes. A master mix of 1X M-MLV RT buffer, 10mM DTT, 1mM dNTPs, 10 units RNasein (Promega), and 200 units M- MLV RT was added. The completed mixture was incubated at 37°C for one hour, followed by a final incubation at 95°C for 5 minutes. The resulting cDNA was then used for downstream applications or stored at -20°C.

PCR

PCRs were performed with the primers as indicated in Table 1. The PCR was run as follows: 1.5' 94°– [30" 94°– 30" annealing temperature – 30" 72°] x30 – 7' 72°. PCRs were used for verification of primer annealing temperatures prior to use in qPCR reactions and to verify the presence of a mutation. PCRs were run at a total volume of 6.25 uL for verification purposes, and large volume 25 uL when products would be used for subsequent experiments such as cloning or sequencing.

Table 1: Primer sequences and uses

| Primer Name | Sequence | Notes |
|--|---|---|
| U6 F | [GATTAGACCACTTTTACCCGG]GTTT TAGAGCTAGAAATAGCAAGT | [] is guide RNA, rest is U6 vector sequence |
| U6 R | CAAACATTTAGATTTGCAATTC | Reverse primer to generate guide RNA vector for |
| <i>Pnpt-1</i> deletion confirmation F | ACCGTCAGCGTCAGCAATTG | To test for mutation from CRISPR/Cas9 site-directed mutagenesis |
| <i>Pnpt-1</i> deletion confirmation R | TTACCTGAGTTTCATAGGAATTT | To test for mutation from CRISPR/Cas9 site-directed mutagenesis |
| wact-2 F | ATCGTCCTCGACTCTGGAGATG | worm actin; as a loading control |
| Wact-2 R | TCACGTCCAGCCAAGTCAAG | worm actin; as a loading control |
| fzo-1 F | TTTGTGTCGATGTCCCTGCT | qPCR |
| fzo-1 R | GAATCGGAACTCGAGGTCTT | qPCR |

qPCR

qPCRs were performed at 60° annealing temperature unless otherwise indicated. 1X SYBR Green mix (Life Technologies) was used along with the designated primers at a final concentration of 0.2 pmol/uL (Table 1). cDNA was diluted 1:16 in a 20 uL single reaction. Reactions were run in triplicate on a 96 well plate. A standard curve was generated for each primer set; dilutions were made at 1:4, 1:8, 1:16, 1:32, and 1:64. Standard curves used control (L4440) cDNA. This standard curve was then used to generate quantities in the experimental wells and degree of knockdown / knockout calculated via the following equation:

$$\frac{\frac{\text{Avg quantity (knockdown)}}{\text{Avg quantity (control)}}}{\frac{\text{Avg quantity (knockdown actin)}}{\text{Avg quantity (control actin)}}}$$

Lifespan Assays

Lifespan assays were performed using N2 worms along with Cas9 knockout lines 1-2 and 1-9. 10 L4 worms were picked onto four 6 cm plates seeded with OP50 allowed to mature into adults, and lay eggs. This period lasts ~24 hours at which point the adult worms are removed from the plates, and the newly laid eggs allowed to

mature into adults over the next 48 hours. 30 adults were lastly picked onto each of 4 large plates and the assay initiated at day 0.

Worms were transferred daily, or every other day, throughout the duration of the egg laying period (~2 weeks). When the egg-laying period concluded, worms were allowed to remain on the same plate provided sufficient food was present. Animals were considered deceased when no movement was elicited following a gentle prod with the end of a pick. Animals that expired secondary to bagging, exploding, or desiccation on the walls were considered censored, and therefore not included in the final statistical analysis. Each life span analysis was performed in triplicate. Survival analysis was performed using the JMP software. Survival data contains duration times until the occurrence of a specific event – usually failure, in our case death. Survival functions are calculated using the nonparametric Kaplan-Meier method. The analysis accounts for data that needs to be censored as well as specialized non-normal distributions. The software generates a subsequent Wilcoxon score, to determine the statistical significance and test the homogeneity of the estimated survival function across the groups.

PQ and NAC Lifespan Assays

Paraquat (PQ) plates were prepared by adding PQ to NGM + Carbenicillin

plates at a final concentration of 0.05mM. N-Acetyl Cysteine (NAC) plates were prepared by adding NAC to NGM + Carbenicillin plates at a final concentration of 10mM. Lifespan assays were performed using N2 worms as control with animals from Cas9 1-2 and 1-9 knockouts for experimental groups. L4 animals were picked onto four large plates of each [NGM / carb], [NGM / PQ / carb], [NGM / NAC / carb]. Animals were allowed to mature into adults and lay eggs for ~24 hours. The following day, adults were removed leaving only eggs behind. Eggs were allowed 3 days to mature into adults before 120 animals from each strain were picked onto 4 large plates and the assay initiated at day 0. Lifespans were carried out as previously noted.

ROS Assay

Approximately 10 L4 worms from each strain were picked onto NGM / OP50 plates and allowed 24 hours to mature and lay eggs. Adults were removed from the plates the next day. Eggs were allowed to mature into adults over the following 3-day period. Plates were washed with M9 to collect all staged worms. The animals were subsequently washed 3x with M9 to ensure all bacteria was removed. A 96 well plate was prepared per AmplexRed (Life Technologies) manufacturer's instructions, and approximately 50 adult worms were aliquoted into each well. An Abs reading was taken at 540 nm, and an average collected. The assay gauges the amount superoxides

via their conversion to hydrogen peroxide. The readings from control and mutant animals were compared, in JMP statistical software, using a t-test.

Imaging of Mitochondria

L4 worms from each strain (N2 / Cas9 1-2 / Cas9 1-9) were picked onto NGM / OP50 and allowed 24 hours to mature and lay eggs. Adults were removed from the plates the following day. Eggs were given 3 days to mature into adults. Plates were washed with M9 to gather worms. The animals were subsequently washed 3 additional times in M9 to remove any extra bacteria. Whole worms were then fixed in 1% paraformaldehyde and 2.5% glutaraldehyde in 0.05M sodium cacodylate buffer with 0.1M sucrose for 3-4 days. Animals were subsequently placed into a postfix of 2% osmium tetroxide in 0.1M sodium cacodylate buffer and embedded in resin (Embed 812 embedding resin [Electron Microscopy Sciences]). Judy Williamson, of the microscopy core, then obtained slices for imaging with a TEM. Judy Williamson obtained images showing a cross-section in the pharyngeal region for further analysis of any morphological changes to the mitochondria in order to maintain consistency with studies previously performed by Laura Lambert. Fixing, resin embedding, and TEM microscopy was performed by the VCU Department of Anatomy and Neurobiology Microscopy Facility, supported, in part, with funding from the NIH-

NINDS Center core grant (5P30NS047463).

Protein Extraction from *C. elegans*

250 μ l of M9 was aliquoted into an Eppendorf tube. 200 worms were picked and put into the M9. Animals were washed 3 times with M9 and gently spun down for 1 minute in between washes. M9 supernatant was removed leaving worms in 25 μ l of M9. Animals were freeze cracked by alternating 30 seconds in liquid nitrogen and 1 minute in a 42° C water bath; this process was repeated 6 times. 25 μ l of 2X sample buffer was added to the worm solution. Animals homogenized for 2 min in boiling water and put immediately at 95°C for 5 min to inhibit proteases.

Western Blot Analysis

The samples were run on 7.5% sodium dodecyl sulfate–polyacrylamide gel electrophoresis (SDS-PAGE) gel and transferred onto nitrocellulose membranes. The membranes were blocked with 10% nonfat milk in Tris-Buffered Saline Tween-20 (TBST) buffer (20 mM Tris-HCl [pH 7.4], 15 mM NaCl, and 0.05% Tween-20) for 1 hour at room temperature and then incubated in 5% milk containing rabbit anti-

human *pnpt* antibodies (1: 5,000) overnight at 4°C. After incubation, membranes were washed three times (15 minutes each) with TBST, incubated with goat anti-rabbit (1: 5,000) in 1% milk at room temperature, and washed three times (15 minutes each) with TBST. The bands were detected using an enhanced chemiluminescence (ECL) kit (Pierce SuperSignal Pico Kit)

Chapter 3: Results

Generation of PNPase mutant strains

Given reported findings from previous studies performed in knockdown animals, it was decided to repeat similar studies in knockout animals. We aimed to confirm previous knockdown observations. The CRISPR/Cas9 system was used to generate targeted deletions in PNPase. Of the 14 injected worms, 9 individual strains fluoresced with the red co-injection marker. This indicated the injection was successful. These 9 individual strains were recovered and sent for sequencing. Laura Lambert determined that 3 strains had single base pair deletions. Two of these strains, 6 and 9, resulted in a predicted frameshift mutation that induced a premature stop codon, approximately 28 codons downstream. Strain 2, on the other hand, was noted to have a single base pair deletion resulting in a frameshift mutation. Two strains (strain 6 and 9) had identical deletions while strain 2 had a different deletion (Figure 6).

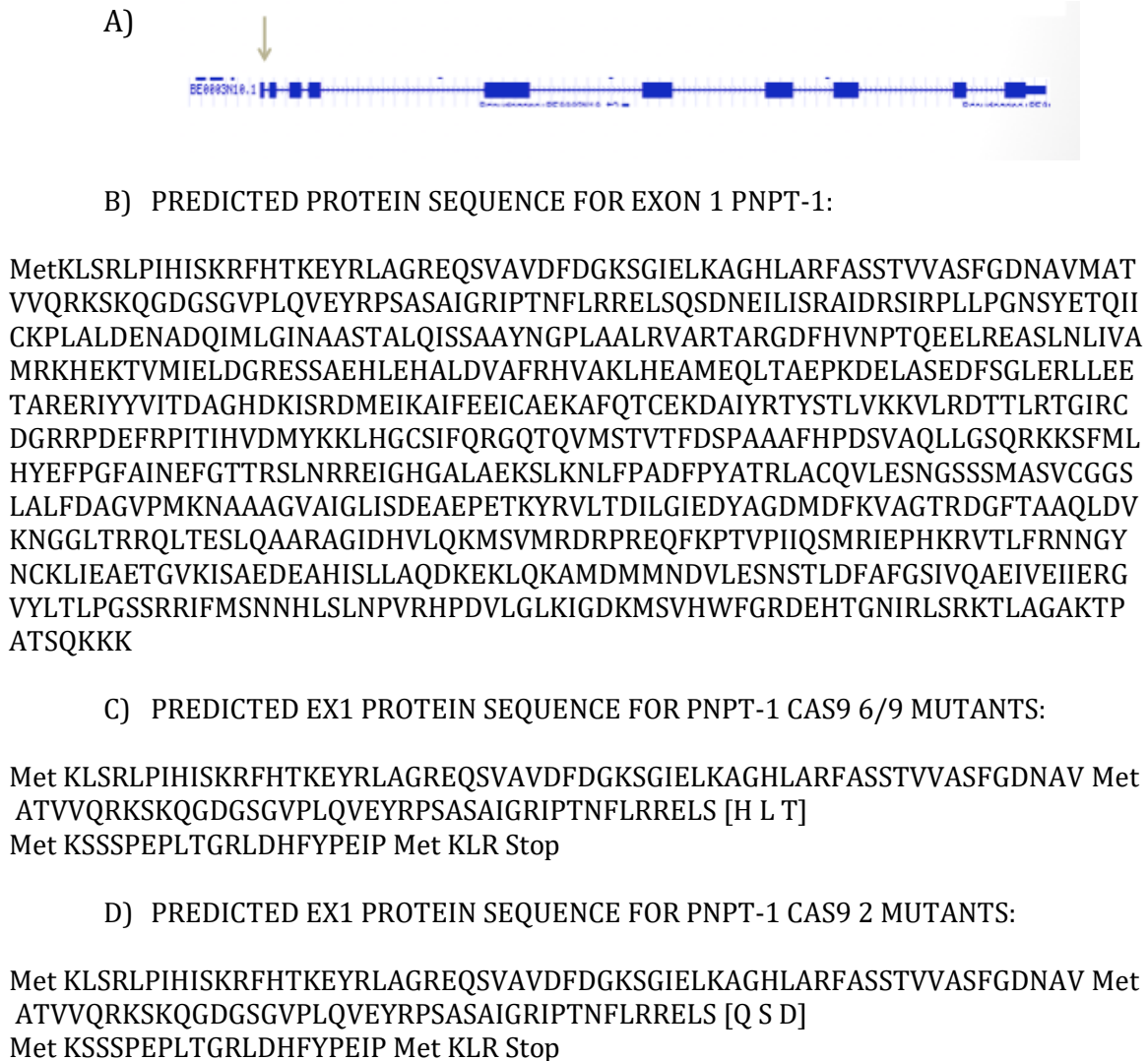


Figure 6: PNPase Deletion strains.

Clones 6 and 9 had identical deletions, resulting in a frameshift and premature stop codon. Clone 2 had a different downstream deletion, also resulting in a frameshift. These deletions are located towards the beginning of the first exon affecting the entirety of the protein's structure. A) Demonstrates the location in the gene of the Cas9 mutation from Laura Lambert's sequencing studies. B) Depicts the correct amino acid sequence of N2 animals. C) Portrays the predicted amino acid sequence for Cas9 6/9 mutant animals. D) Represents the predicted amino acid sequence for Cas9 2 mutant animals.

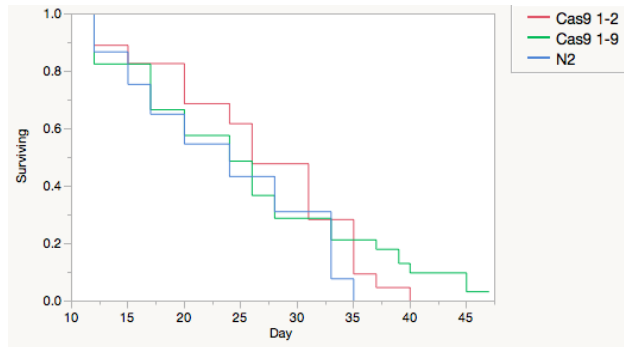
Validation of PNPase knockout via western blot analysis

Six attempts were made to verify the *pnpt-1* knockout and knockdown via western blot analysis. No successful data was obtained. No protein bands were visualized in the gel. Rather, a large amount of protein was visible, at the top of the gel, in their original wells. Multiple attempts were made to re-extract the protein according to the lab's protocol with no success. Subsequent troubleshooting methods were attempted with failure. An additional protocol was received from Dr. Kari Messina at William and Mary College; the new method was attempted without success. Further studies were pursued while additional western blot methods were reviewed. One method reviewed, but not attempted was extraction using sea salt previously described by Harris et. al., 2016.

Characterization of Lifespan of PNPase knockout in *C. elegans*

Previous studies found an increased lifespan of knockdown animals when grown on NGM / OP50. Additional experiments observed no further extension of lifespan when knockdown animals were grown on medium prepared with Paraquat (PQ), a known superoxide generator. Furthermore, studies showed an abolishment of this lifespan extension on plates made with NAC, a known antioxidant. Similar

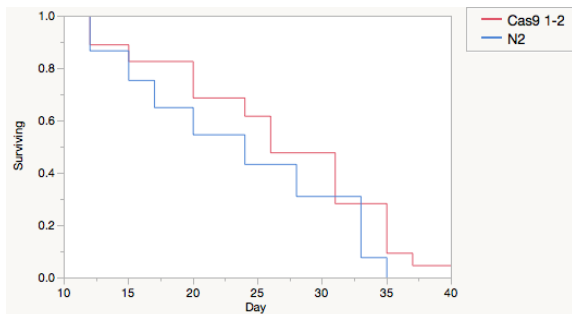
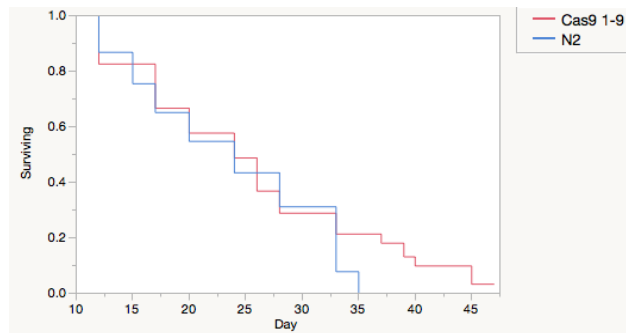
experiments were performed to determine if the findings were validated across the developed knockout lines. An initial study was performed using only NGM with OP50 bacteria to obtain a baseline lifespan across the N2 animals along with the Cas9 1-2 and 1-9 knockout lines. It was found that the lifespan in the knockout animals 1-2 was minimally, but significantly, extended (Figure 7, Table 3). Furthermore, no observable extended lifespan was found in Cas9 1-9 knockout animal lines.

Trial A**Figure 7: PNPase knockout extends lifespan in *C. elegans*.**

A single study was completed in order to determine a baseline lifespan over the N2 (control) and Cas9 1-2 and Cas9 1-9 knockout lines. Knockout animals (1-2 / 1-9) demonstrate an extended lifespan when compared to control animals (N2).

Table 2: Mean lifespans and p-values for trial as seen in figure 7

| Trial: | Mean Lifespan | p-value: |
|--------------------|----------------------|-----------------|
| A: N2 | 23.7 days | |
| A: Cas9 1-2 | 26.7 days | |
| A: Cas9 1-9 | 25.4 days | 0.05 |

Trial B**Trial C****Figure 8: PNPase knockout extends lifespan in *C. elegans*.**

When analyzed separately, it was found that (B) knockout animals Cas9 1-2 demonstrate an extended lifespan as compared to control animals (N2). It was further demonstrated that (C) the knockout line Cas9 1-9 animals do not share this same significant lifespan extension.

Table 3: Mean lifespans and p-values for trials B-C as seen in figure 8

| Trial: | Mean Lifespan: | p-value: |
|--------------------|-----------------------|-----------------|
| A: N2 | 23.7 days | |
| A: Cas9 1-2 | 26.7 days | 0.03 |
| B: N2 | 23.7 days | |
| B: Cas9 1-9 | 25.4 days | 0.72 |

Confirmation of PNPase lifespan extension via an increase in ROS

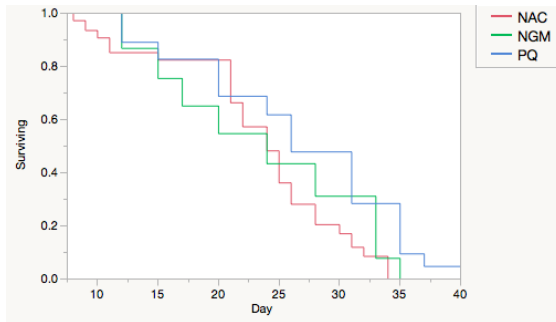
Reactive oxygen species (ROS) are derived from superoxides, which are generated when oxygen is reduced. This most commonly occurs in Complex III of the respiratory chain, which releases superoxides into the intermembrane space of the mitochondria. Multiple mechanisms in place have the ability to counteract the effect of these superoxides. The primary mechanism utilizes superoxide dismutases (SODs). SODs convert the superoxide into hydrogen peroxide, which can subsequently be eliminated by a variety of other peroxidases (Sena and Chandel, 2012). Recent studies demonstrate that a slight increase in ROS may activate beneficial stress responses in animals, causing an extension in lifespan (Schulz et. al, 2007; Zarse et al., 2012).

To determine if a PNPase knockout extends lifespan via an increase in ROS, lifespans were performed using knockout and control animals on NGM with either the superoxide generator paraquat (PQ) or the antioxidant NAC.

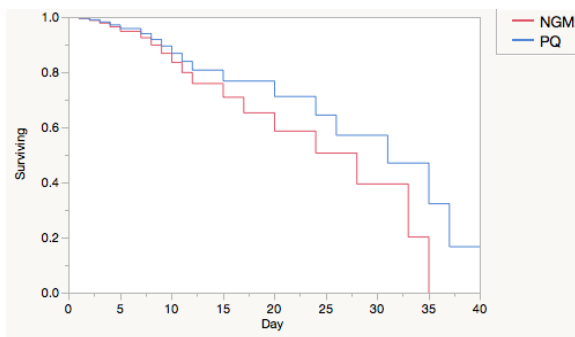
The PQ concentration used (0.05mM) was sufficient enough to extend the lifespan of control animals (Figures 12, 13, 14). Additionally, it was noted that the PQ concentration had no significant increase on lifespan in *pnpt-1* knockout animals 1-2 and 1-9. Conversely, NAC is known to reduce the amount of ROS. Knockout animals

showed a reduction in lifespan, sometimes surpassing that of the control animals. This would suggest that the lifespan extension in *pnpt-1* knockout animals was potentially caused by an increase in superoxides buildup.

A:



B.



C.

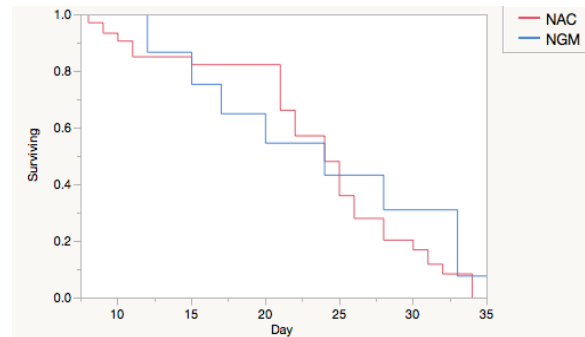


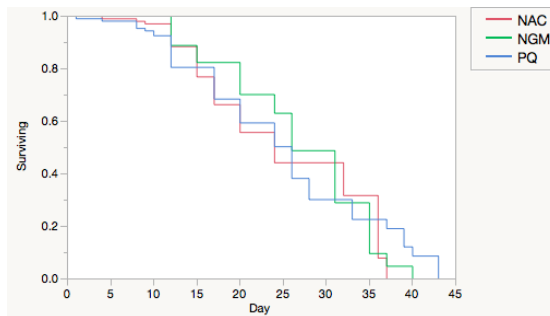
Figure 9: N2 animals exhibit lifespan extension on PQ, but not on NAC

(A) Survival analysis representative of N2 animals grown on NGM, PQ, and NAC. (B) N2 animals grown on PQ demonstrated an extended lifespan as compared to those grown on NGM. (C) N2 animals grown on NAC showed no significant extension from N2 animals grown on NGM.

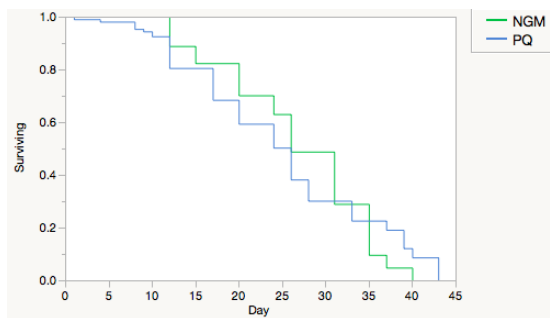
Table 4: Mean lifespans and p-values for triplicate N2 trials A-C as seen in figure 9

| Trial: N2 | Mean Lifespan | p-value w/ NGM: |
|------------------|----------------------|------------------------|
| A: NGM | 23.7 days | |
| A: PQ | 27 days | 0.001 |
| A: NAC | 23.2 days | 0.98 |

A:



B:



C:

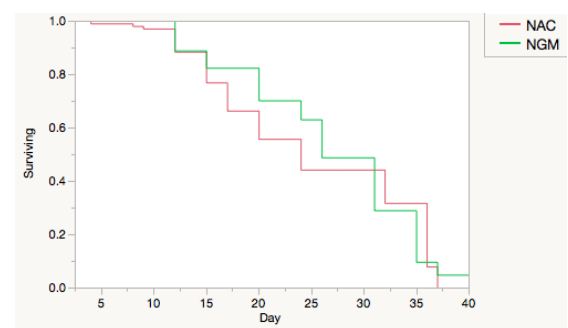


Figure 10: Cas9 1-2 knockout lifespans on PQ / NAC

(A) Survival Analysis representative of Cas9 1-2 animals grown on NGM, PQ, and NAC.
 (B / C) Cas9 1-2 knockout animals grown on PQ or NAC demonstrated no significant lifespan extension as compared to knockout animals grown on NGM.

Table 5: Mean lifespans and p-values for triplicate Cas9 1-2 trials A-C as seen in figure 10

| Trial: 1-2 | Mean Lifespan | p-value w/ NGM: |
|-------------------|----------------------|------------------------|
| A: NGM | 26.7 days | |
| A: PQ | 25.1 days | 0.06 |
| A: NAC | 25.2 days | 0.21 |

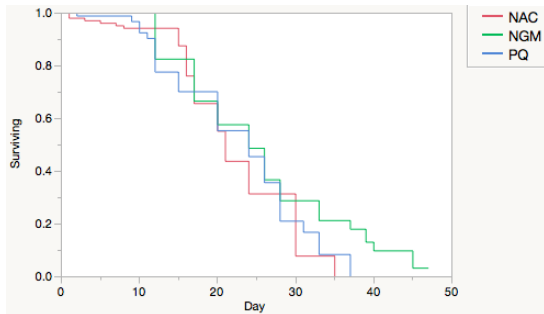
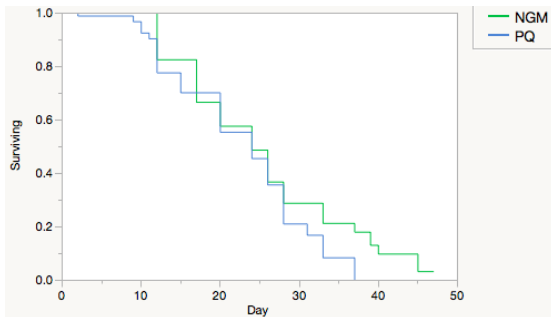
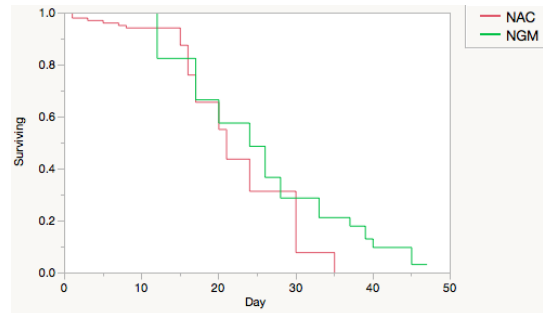
A:**B:****C:**

Figure 11: Cas9 1-9 knockout lifespans on PQ / NAC

(A) Survival Analysis representative of Cas9 1-9 animals grown on NGM, PQ, and NAC.

(B / C) Cas9 1-2 knockout animals grown on PQ or NAC demonstrated no significant lifespan extension as compared to knockout animals grown on NGM.

Table 6: Mean lifespans and p-values for triplicate Cas9 1-9 trials A-C as seen in figure 11

| Trial: 1-9 | Mean Lifespan | p-value w/ NGM: |
|-------------------|----------------------|------------------------|
| A: NGM | 25.4 days | |
| A: PQ | 22.7 days | 0.32 |
| A: NAC | 22.1 days | 0.26 |

Quantification of ROS in *pnpt-1* knockout animals

Previous knockdown studies in *C. elegans* reported the animals had a measurable and significant increase in ROS as compared to control animals. It was thought that the *pnpt-1* knockdown increases ROS production, which leads to a downstream increase in lifespan. Our aim was to repeat these studies in hopes of confirming an increase in the level of ROS across the knockout strains. ROS production was measured with use of the AmplexRed assay. This assay measures the total amount of superoxides via their conversion to hydrogen peroxide and quantified them by comparing absorbency. It was found that the knockout groups both demonstrated a significant decrease in ROS production as compared to the control group. This was contrary to findings from earlier studies in knockdown animals.

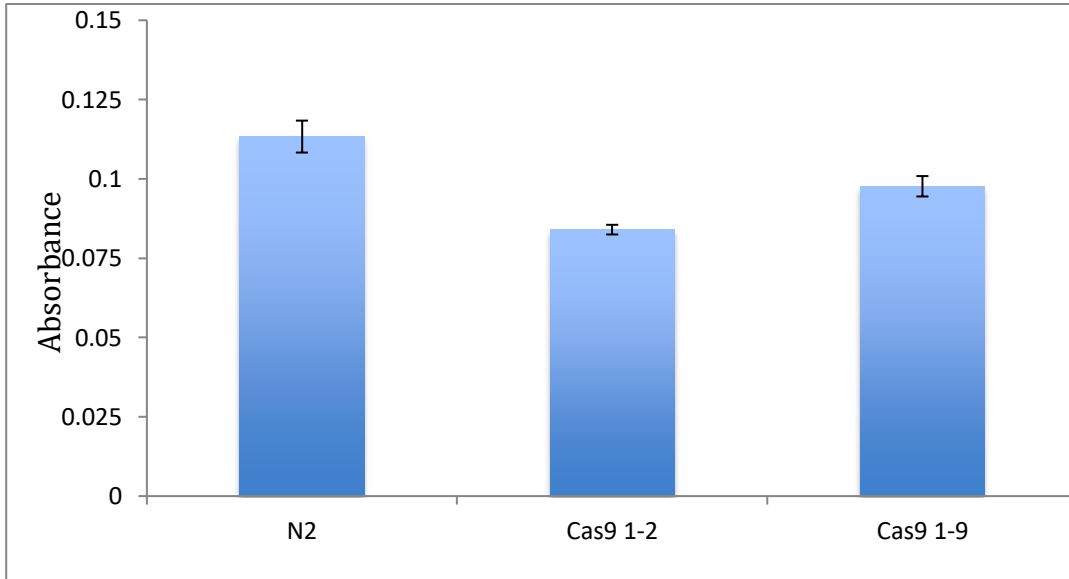


Figure 12: PNPase knockout and ROS production.

pnpt-1 knockout decreases ROS production when compared to control over 3 trials.
p-value 1-2 = 0.002; p-value 1-9 = 0.02

PNPase knockout does not affect mitochondrial structure

Prior studies, performed by Laura Lambert, in PNPase knockdown animals used transmission electron microscopy (TEM) to further investigate any potential physical changes in the mitochondria. Laura Lambert's studies demonstrated that the *pnpt-1* animals had significantly larger mitochondria as compared to control animals. These studies, however, found no observable difference in the cristae of the knockdown mitochondria when compared to the control. We obtained additional images of both control and knockout animals using TEM, with the hopes of validating previous data. We found no significant distinction between the mitochondrial size of control animals and knockout animals. Furthermore, this study's findings were confirmed using a t-test (Figure 14). These findings were contrary to our hypotheses given previous studies.

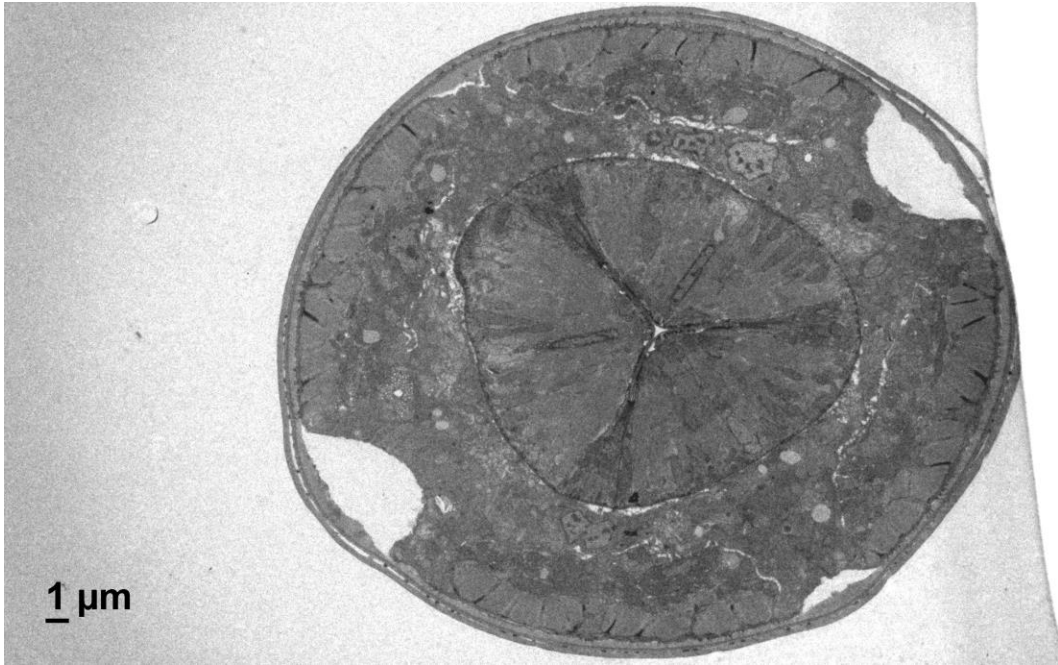


Figure 13: cross section TEM image of N2 animal

Control and knockout animals were fixed and cross-sectioned just superior to the Metacorpus (anterior bulb) of the pharynx. The mitochondria were examined under TEM.

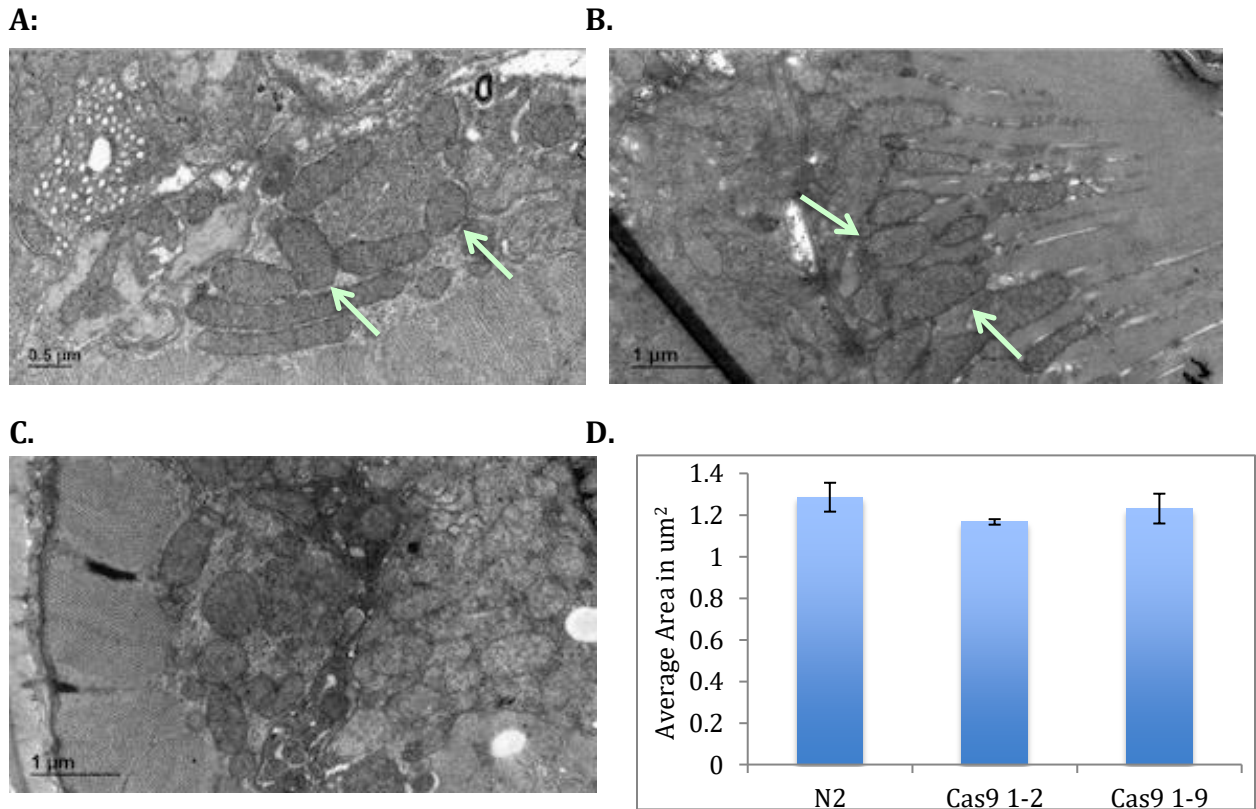


Figure 14: *pnpt-1* knockout does not affect mitochondrial size as previously reported in knockdown studies.

A, B, and C) TEM images of mitochondria from control N2 (A) animals, knockout lines Cas9 1-2 (B), and Cas9 1-9 (C) at 30000X. 6 animals from each line were imaged and 12 mitochondria from each animal measured; N=72 total mitochondria. Knockout animals showed no significant difference in the size of the mitochondria as compared to the control group; p-value 0.2398 (N2/1-2) and p-value 0.5187 (N2/1-9). Green arrows indicate the mitochondria. (D) Visual representation of average mitochondrial area across the reported lines.

PNPase knockout and *fzo-1* expression

Mitochondrial fusion proteins mfn-1 and mfn-2 are other known targets of ROS in humans. Mitochondria are highly dynamic organelles with a morphology that is largely determined by the equilibrium between fission and fusion events (Cao et. al.). According to previous studies, an increase in ROS increases the downstream expression of these proteins, which subsequently leads to an increase in mitochondrial fusion.

Mitofusin-1 and Mitofusin-2 are GTPases located in the outer membrane and essential for mitochondrial fusion. Former studies showed a decrease in membrane potential of mouse cells with mutations in mfn-1 (Chen et. al., 2005). *Fzo-1* is the worm homolog of mfn-2. Studies from a former student in this lab demonstrated an increase in *fzo-1* transcript amongst knockdown animals. Given the concerning findings in mitochondrial sizes between control and knockout groups, it was decided to repeat studies on *fzo-1*. Further investigation demonstrated a 2-fold over expression in *fzo-1* Cas9 1-2 knockout animals, but no significant changes in Cas9 1-9 knockouts (Figure 15). Following these findings, it was decided to resequence the knockout lines to ensure a mutation was present (Figure 16).

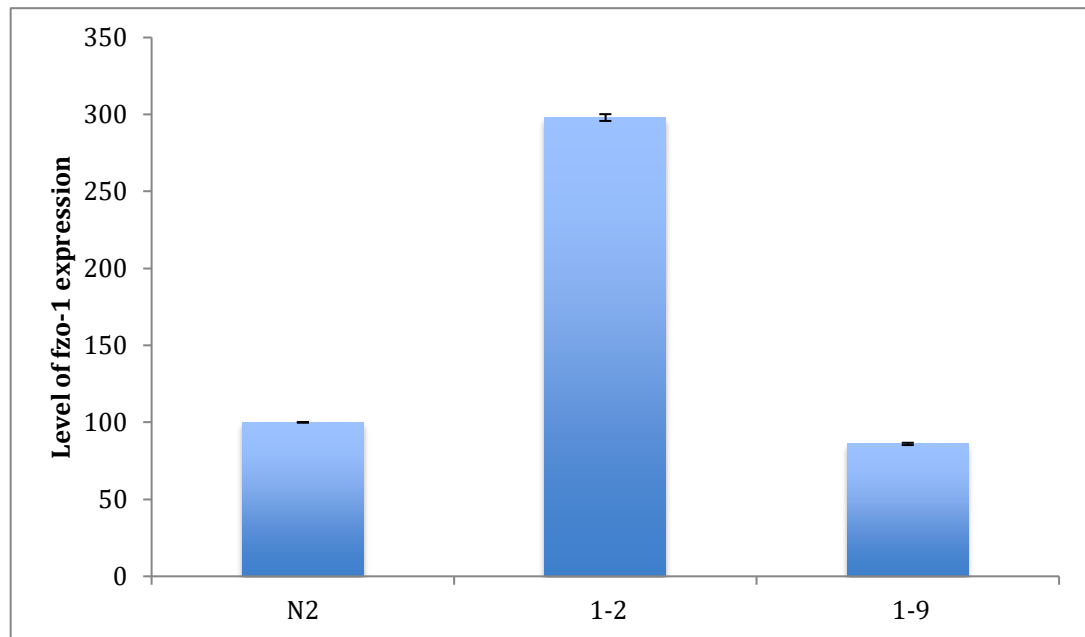


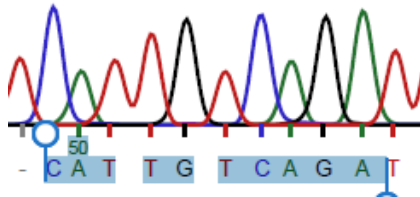
Figure 15: PNPase knockout and *fzo-1* expression

Level of *fzo-1* expression was increased almost three-fold in knockout lines 1-2 as compared to control (N2) and knockout line 1-9.

Resequencing of PNPase knockout animals

Given the contradictory findings, between our studies and those previously performed by Laura Lambert, we decided to resequence all animal lines to ensure the mutations still existed. On further evaluation, it was determined that no mutation was present across both knockout lines. Review of Laura's initial sequencing documents shows a mutation in the forward sequence; however, no mutation was present in the reverse compliment. All subsequent studies were postponed indefinitely.

A:



B:

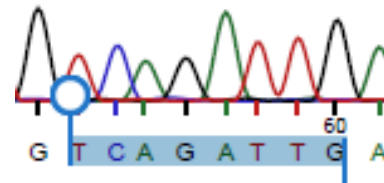


Figure 16: Resequencing of PNPase knockout animals

Resequencing of the PNPase knockouts demonstrate no mutation present when compared to N2 sequencing studies. A) depicts the area of knockout in question for Cas9 1-2 while B) depicts the area of knockout in question for Cas 9 1-9. Both sequencing studies reported normal sequences without evidence mutation.

Chapter 4: Discussion

This study was performed, in *pnpt-1* knockout animals, in an attempt to determine the effect of whole animal PNPase knockout. We furthermore, aimed to determine the validity of previous conditional knockdown studies. Previous experiments in mice demonstrated whole animal knockouts were embryonic lethal. These studies highlighted the crucial role PNPase plays throughout early mammalian development (Wang et. al., 2010).

Given the contradictory and unexpected results we were observing it was decided to resequence the Cas 9 1-2 and Cas 9 1-9 knockout animals. Our resequencing study reported no evidence of a mutation across any of the knockout lines. On reevaluation of Laura Lambert's initial sequencing results no mutation was found on the reverse compliment strand. While much headway has been made with CRISPR / Cas 9 in recent years, it is only predicted to have 90% efficiency. One caveat to the CRISPR / Cas 9 system is the potential for off-target effects. While Cas9 is ideally directed to its binding site by a sgRNA, with close to 100% specificity to the desired target, off-target effects can, and do, occur. This may give rise to unintentional downstream effects, which may confound conclusions of the studies. On further analysis, the 21bp sgRNA sequence used for our Cas9 site directed mutagenesis was

predicted to bind to greater than 300 additional sites in the *C. elegans* genome. Thus, an unknown off-target mutation is the most likely explanation for our skewed results. However, not having a defined *pnpt-1* mutation does not explain our noted decrease in ROS production and the lack of morphological changes to the mitochondria.

Studies performed in *C. elegans*, by Laura Lambert, allowed for the use of a bacterial RNAi system to create a knockdown of *pnpt-1*. This RNAi system permitted a lower level of expression lest PNPase was also necessary for development in *C. elegans*. Throughout Laura Lambert's previous trials, it was observed that the PNPase knockdown significantly extends lifespan when the knockdown was present from oocyte formation. It was thought this might indicate that the causative mechanism for lifespan extension lies in an early stage of development.

Laura Lambert additionally conjectured that an increase in ROS, such as superoxides or the hydroxyl radical, may lead to an increase in lifespan extension. Laura utilized animals with known mitochondrial mutations for additional lifespan studies. She hypothesized that, in known *nuo-6* and *isp-1* mutant lines, an increase of superoxides can activate downstream mechanisms to slow aging at the level of gene expression (Lambert, 2015). Furthermore, the introduction of NAC, a known anti-oxidant, into the medium abolishes the lifespan observed in *nuo-6* and *isp-1* mutants,

while Paraquat (PQ) a superoxide generator demonstrates no further extension. Laura Lambert found that the lifespan extension in PNPase knockdown animals modeled that of nuo-6 and isp-1 mutants, indicating potential for an OXPHOS and/or ROS production link (Lambert, 2015).

To better determine the effects of PNPase on ROS production we performed lifespans, with knockout animals, on NGM, PQ, and NAC mediums. Our studies aimed to determine if combining the differing mediums with PNPase knockout animals would have an effect on the lifespan extension previously observed. We concluded that PQ animals showed no further lifespan extension than the knockdown animals although it did extend the lifespans of the control animals. Furthermore, NAC was found to reduce the lifespan of the knockdown animals similar to that of the control group. NAC was not observed to show any additional effects on the control animals.

Increased ROS production is mostly believed to be detrimental and fatal to an organism. More recent studies, however, suggest that a slight increase in ROS may actually help to activate a beneficial stress response in animals. This stress response is subsequently the cause of the noted lifespan extension (Schulz et. al., 2007; Zarse et. al., 2012).

The lifespan extension observed, in knockdown animal studies performed by Laura Lambert, was thought to be driven, in part, by an increase in ROS that was secondary to a stress-mediated response in *C. elegans*. She performed subsequent tests to better measure the affect ROS accumulation may play on life span extension. The assay Laura Lambert used measured the conversion rate of superoxides to hydrogen peroxide.

Our studies in the predicted mutant lines reported a significant extension of lifespan in Cas9 1-2 animals, but no extension in the 1-9 line. As we know there was no confirmed mutation, however, we would expect the predicted knockout animals to behave similar in fashion to the N2 animals. Furthermore, KD animals demonstrated a 50% increase in ROS production that was thought to drive the observable lifespan extension. Neither knockout line 1-2 nor 1-9 demonstrated similar findings. Contradictory, both knockout lines exhibited a decrease in ROS production. This was most likely secondary to an unknown off-target mutation. However, given these findings it is hard to correlate lifespan extension with an increase in ROS. What we previously thought was a driving mechanism to the noted lifespan extensions may be only one of multiple factors to play a role in longevity. Additional sequencing of either the whole genome, or selected loci, would need to be performed on these animals to confirm any off-target mutations.

Prior *C. elegans* work has shown an increase in the density of the mitochondrial networks of animals with mitochondrial defects (Lee et. al., 2003). Supplementary studies, from this lab, imaged individual mitochondria of knockdown animals along with the mitochondrial network. Increased network size was found in knockdown animals as compared to the control group. Furthermore, knockdown animals were observed to have larger mitochondria. This could be indicative of a possible dysfunction of the fission and fusion rate in mitochondria. This rate is highly regulated as the integrity of the mitochondria, and the cell, depend on it. The rate of mitochondrial fusion is mediated by mfn-1 and mfn-2. The worm homolog of mfn-2, *fzo-1*, was found mitochondrial fusion (Robb et. al., 2013). Findings from this lab further indicated the increased level of *fzo-1* as a potential mechanism for the previously observed changes to the mitochondrial network along with the noted dysmorphic mitochondria. Additional imaging and statistical analyses was performed using the control group (N2) and knockout lines. No observable changes were noted between the groups. Statistical analysis further confirmed no significant changes amongst the control and knockout animals. This was another point of concern as these findings were not to be expected.

In order to maintain homeostasis and better regulate cellular processes, including ROS and ATP production, the mitochondria must regularly fuse and divide

(Archer, 2013). Fusion is known to help limit the ramifications of cellular stress by allowing the contents of damaged mitochondria to blend with the contents of undamaged mitochondria (Youle, 2012). Previous studies in HO-1 melanoma cell lines report finding filamentous and granular mitochondria with a decreased membrane potential and a decrease in the enzymatic activity of the respiratory chain (Chen et al. 2006). Given we observed no significant change to the mitochondria between control and knockout animals our observed increase in *fzo-1* transcript in the Cas9 1-2 line was intriguing. This would give rise to the idea that changes in *fzo-1* transcript levels and mitochondrial morphology was not correlated as previously thought. It would be beneficial to further study levels of *drp-1*, the mitochondrial fission protein, in the 1-2 line. The Cas9 1-2 animals may potentially demonstrate an increase in both fission and fusion proteins which would explain why no observable morphological changes could be found in the alleged knockout animals. We would not expect a need for increased fusion rates given the otherwise healthy appearing state of the mitochondria in the knockout lines. However, our mitochondria conclusions do draw a parallel to our Cas9 1-2 *fzo-1* findings.

Additional studies are required to confirm the effects of *pnpt-1* mutations on lifespan analyses. Furthermore, repeat studies will present potential for validation of prior knockdown experiments. Testing for similar findings across multiple other

known mitochondrial mutants would also be beneficial in helping to determine mechanisms specific to *pnpt-1*. Further investigation into the stress responses of *C. elegans* may help to better link PNPase knockout, increased ROS, and extended lifespan. It would be interesting to note whether or not alternative types of stressors have differing effects on *pnpt-1* knockout animals and ROS production.

fzo-1 upregulation in addition to the increased size of mitochondria presents the possibility of an underlying mechanism that helps to elude downstream cellular stress caused by a mutation in *pnpt-1*, thus extending the lifespan. This was not apparent in the Cas9 1-2 and Cas9 1-9 lines. However, there is a large amount of support to implicate disordered mitochondrial dynamics as a contributing factor to more complex disease such as cancer or neurodegeneration. Cancer cells have previously been found to show an increase in mitochondrial fragmentation (Archer, 2013).

A PNPase knockdown has yet to be found associated with a cancerous phenotype. However, mutations in the human gene are known to cause phenotypes similar to those of other mitochondrial disorders. These cover a variety of complex presentations that include but are not limited to hearing loss and other neuropathies. Familial studies, involving multiple families, demonstrated the importance of PNPase

when it comes to the import of small RNAs in overall mitochondrial function. Further investigation into the individual families would be necessary to determine whether or not there are other possible mechanisms. (Vedrenne et. al., 2012; Ameln et. al., 2012). Upon further investigation, new evidence can be used to help generate and manage treatment plans for all of the associated disorders previously listed.

In light of secondary sequencing analyses all data was considered inconclusive. All studies will need to be replicated for further validation. To start a confirmed mutant of PNPase needs to be generated. The CRISPR system remains a valid option for mutagenesis with modifications to the original approach. New primers should be designed and verified to minimize off target effects. N2 animals will need to be re-injected and new mutant lines confirmed. Subsequent sequencing will need to be performed and verified prior to repeating all experiments previously described in this and Laura Lamberts theses.

CHAPTER 5: Appendix - Glucose intolerance in *C. elegans* and its effects on Lifespan

INTRODUCTION

Wolfram syndrome 1 (WS1) is an autosomal recessive disorder characterized by Diabetes Insipidus, Diabetes Mellitus, Optic Atrophy, and Deafness (DI, DM, OA, D) and is associated with other variable clinical manifestations. The causative gene for WS1 (*WFS1*) encoding the protein Wolframin can be found on chromosome 4p16.1. Wolframin has an important function in maintaining the homeostasis of the endoplasmic reticulum (ER) in pancreatic β cells (Rigoli et. al., 2012). More recently, another causative gene, *CISD2*, has been identified in patients with a type of Wolfram syndrome (WS2) resulting in early optic atrophy, diabetes mellitus, deafness, and decreased lifespan, but not diabetes insipidus. The *CISD2*-encoded protein ERIS (endoplasmic reticulum intermembrane small protein) also localizes to ER, but does not interact directly with wolframin (Amr, 2010).

Diabetes mellitus is a group of autoimmune diseases characterized by defects in insulin secretion resulting in hyperglycemia. There are two primary types of diabetes. Individuals diagnosed with type 1 'Juvenile' diabetes are incapable of producing pancreatic insulin and must rely on insulin for survival. Individuals diagnosed with type 2 'adult onset' diabetes either produce inadequate amounts of

insulin or are insulin resistant. These individuals therefore, can often manage their symptoms with medication and an appropriate diet. Over time, diabetes can lead to kidney failure, blindness, neuropathy, atherosclerotic changes, and death. The disease is the third leading cause of death in the United States after heart disease and cancer (Genuth et. al, 2003).

Caenorhabditis elegans (*C. elegans*) is a free-living, non-parasitic soil nematode that can be safely used in the laboratory and is common around the world. These animals are small (about 1 mm in length), transparent, feed on bacteria such as *E. coli*, and are easy to manipulate. They are cheaply housed and cultivated in large numbers (10,000 worms/petri dish) in the laboratory. Furthermore, the *C. elegans* complete genome has been sequenced and the developmental lineage of each cell is known. For these reasons, they are good model organism for study. *C. elegans* has five pairs of autosomes and one pair of sex chromosome (Horvitz et. al. 1997). It has two sexes, hermaphrodites and males. Sexual determination in *C. elegans* is similar to *Drosophila*; the ratio of sex chromosomes to autosomes determines its sex. If the 6th chromosome pair is XX, then *C. elegans* will be a hermaphrodite. A XO combination in the 6th chromosome pair will produce a male. Hermaphrodites can self-fertilize or mate with males but cannot fertilize each other. In nature, hermaphrodites are the most common sex. When hermaphrodites mate with males, 50% of the progeny will be males and 50% will be hermaphrodites. In the laboratory, self-fertilization of

hermaphrodites or crossing with males can be manipulated to produce progeny with desired genotypes that are especially useful for genetic study (Horvitz et. al. 1997). In addition, *C. elegans* are extremely fecund; a hermaphrodite can produce about 300 to 350 offspring under self-fertilization and more if it mates with males. These traits make it easy to produce numerous genotypes and phenotypes for genetic research (Horvitz et. al. 1997).

C. elegans is usually grown monoxenically in the laboratory using *E. coli* strain OP50 as a food source. *E. coli* OP50 is an uracil auxotroph whose growth is limited on NGM plates. A limited bacterial lawn is desirable because it allows for easier observation and better mating of the worms (Stiernage et. al. 2013).

Our aim was to establish *Caenorhabditis elegans* as a model for glucose intolerance and toxicity –mediated life span reduction. To better understand the effects that glucose intolerance might have on the average lifespan *C. elegans* was used as a knockdown model for the *CISD2* ortholog (wCISD2) in worms. Gene knockdown refers to a process by which the expression of a specific gene can be experimentally reduced in an organism. Double stranded RNA (dsRNA), within a cell, initiates a complex response mechanism which includes a downstream cascade of RNA interference (RNAi) events. In this sequence Dicer, a cellular enzyme, binds to the dsRNA and cleaves it into smaller fragments of approximately 20 nucleotides; these are known as small interfering RNA. (siRNA). These RNA pairs bind to a cellular

enzyme called RNA-induced silencing complex (RISC) that uses one strand of the siRNA to bind to mRNA of complementary sequence. The nuclease activity of RISC then degrades the mRNA, thus silencing expression of the gene. Similarly, the genetic machinery of cells is believed to utilize RNAi to control the expression of endogenous mRNA, adding a new layer of post-transcriptional regulation. RNAi can be utilized to knockdown target genes of interest with high specificity and relative ease (Mocellin et. al. 2004). As we wish to recreate conditions in *C. elegans* similar to that of glucose concentrations in diabetic patients under poor glucose control, whole-body extract of 10–15 mmol/L was used as a baseline and all subsequent glucose calculations were derived from these numbers (Schlotterer et. al. 2014). In order to induce a knockdown for the *wCISD2* gene, worms are grown on plates with a bacterial lawn containing a plasmid WC-22. When inserted into the vector L4440 the WC-22 plasmid induces a knockdown of the *wCISD2* gene. This leads to a degradation of the mRNA and subsequent discontinued production of the protein.

Glucose restriction has been found to extend *C. elegans* life span, whereas, in contrast, high glucose concentrations have been previously shown to reduce life span. With an RNAi induced knockdown for *wCISD2* a significantly shortened lifespan was hypothesized (Schlotterer et. al. 2013).

MATERIALS AND METHODS

***C. elegans* maintenance**

Initial worm plates were maintained through a process known as ‘chunking’. Plates were labeled with the date of chunking along with strain of worm and type of bacteria seeded. *C. elegans* were grown on NGM plates seeded with 100ul of OP50 bacteria and maintained at 20°C. A small “chunk” was cut from an existing plate of animals and transferred, face down, to the new plate. All subsequent plates were chunked from these original plates. CF3152 animals, gifted from Dr. Malene Hansen, were chunked between every 3-5 days for routine maintenance.

Bleaching of adult *C. elegans*

When plates of worms became contaminated with mold or bacteria, it was necessary to bleach the worms and transfer them to a new, clean plate. A bleach solution was made using 30% bleach with 0.6 N KOH and filter sterilized. On a fresh NGM + OP50 plate, a 20 uL aliquot of bleach solution was pipetted along the edge of the plate. Between 5 and 10 gravid, contaminated animals were picked and placed directly into the solution. The animal’s cuticles were ruptured by the bleach solution allowing the eggs to be freed from within. Eggs were allowed to mature in incubation at 20°C face up, overnight. The following day, L1 larvae were transferred to a new plate.

DNA Extraction from *C. elegans*

12 adult worms were picked into 20 μ L of worm lysis buffer (WLB) with freshly added proteinase K at a concentration of 60 ng/ μ L. The worm solution was frozen at -80°C for 10-15 minutes, and then incubated at 65°C for 1 hour to allow for lysis of the cuticle membrane. A 15-minute incubation at 95°C was used to inactivate the proteinase K. DNA was stored at -20°C . WLB consists of: 10 mM TRIS (pH 8.0), 50 mM KCl, 2.5 mM MgCl_2 , 0.45% Tween 20, 0.45% NP-40, and 0.05% gelatin.

RNA Extraction from *C. elegans*

Worms grown on 15-20 6 cm plates were washed off with 5 mLs M9 and collected in a 15-mL conical tube. The worms were gently pelleted at 1000 rpm for 5 minutes, and the supernatant discarded. Worms were subsequently washed 3 additional times, in the same manner, using 5 mLs M9 for each wash. After the last of the supernatant was removed, 200 μ L Trizol reagent was added. Worms were then freeze-cracked by alternating 30 seconds in liquid nitrogen and a 1-minute thaw at 37°C ; this was repeated approximately 7 times. The Trizol/worm mixture was transferred to a 1.5 mL Eppendorf tube, 200 μ L chloroform was added and spun at 13,000 rpm, at 4°C , for 15 minutes. The aqueous fraction was transferred to a new 1.5 mL tube, and an equal volume of 70% isopropanol was added. A Qiagen RNA prep kit

was used to purify the RNA following the manufacturer's instructions. RNA that was not immediately used for subsequent experiments was stored at -80°C.

Generating cDNA from *C. elegans* RNA

The following was added to a 0.7 mL tube: 1ug of total RNA, 100 ng oligo dT primer, 100 ng random primers, and DEPC H₂O to 12 uL. The RNA was incubated at 70°C for 10 minutes. A master mix of 1X M-MLV RT buffer, 10 mM DTT, 1 mM dNTPs, 10 units RNasein (Promega), and 200 units M- MLV RT was added. The reaction was incubated at 37°C for one hour, followed by a final incubation at 95°C for 5 minutes. The resulting cDNA was then used for downstream applications or stored at -20°C.

RNAi

RNAi was introduced by feeding the animals bacteria expressing dsRNA. dsRNA expression was induced by growing overnight bacterial cultures at 37°C in LB (+Ampicillin to 100 ng/uL). The overnights were diluted 1:100 in fresh LB Ampicillin (final concentration of 100 ng/uL) and incubated in a 37°C shaker, at 225 rpm, for 3 hours. IPTG was added to a final concentration of 0.4 mM and returned to the 37°C shaker for 2 hours. Additional Ampicillin was added to a final concentration of 100 ng/uL along with a second dose of IPTG to a final concentration of 0.4 mM. Plates were then seeded with 100 uL bacteria (6 cm plate) or 400 uL (10 cm plate).

Lifespan Preparation

A 1M glucose solution was prepared, autoclaved and allowed to cool to room temperature. A Nematode Growth Medium (NGM) was prepared and autoclaved. Post sterilization, Carbenicillin (carb) (25 µg/ml) and an aliquot of 1M Glucose solution (40 ml/L) were added to the media bringing the final concentration of the glucose agar to 40 mmol/L of solution. A 10-ml pipette was used to pour 50 large glucose agar plates with 20 mL of media each, while a lighter was used to remove any bubbles.

Bacterial cultures (WC-22 or L4440) in LB amp (100 µg/mL) were incubated in a shaker at 37°C overnight. Following overnight incubation each culture was diluted 1:100 in the specific LB volume needed for seeding. Supplementary amp was added (100 µg/mL) and the culture was incubated in the shaker for an additional three hours. IPTG (1M) was added to a concentration of 0.4 mM and the culture was incubated for a final two hours. Following the final incubation 400 ul of culture was seeded onto each of the 50 glucose plates (25 plates per bacterial line).

In preparation for lifespans, WC-22 and L4440 overnight cultures were prepared as previously noted and seeded in aliquots (100ul) onto medium carb plates. To obtain enough eggs of the same initial age 10 worms (L3 or L4) were picked onto plates. Two plates were picked per plasmid totaling 20 worms each. After an overnight growth period, all adult worms were picked off the plates leaving only eggs (at least 120 per plasmid line) to grow. The plates were kept at 20°C for 48 hours

while the eggs fully matured. At this point 15 adult worms were picked and placed onto a large glucose plate containing the WC-22 or L4440 bacterial plasmid, 8 plates were picked per plasmid totaling 120 worms per line. The worms were transferred to new glucose plates containing the same plasmid every day until they ceased to lay eggs. The death rates of each worm were carefully observed and noted. Animals were considered deceased when no movement was observed following a gentle prod with the end of a pick. Animals who died of extraneous circumstances, such as bagging or exploding, were considered 'censored' and not included in the statistical analyses. Survival analysis was performed using the JMP software. Survival data contains duration times until the occurrence of a specific event – usually failure, in our case death. Survival functions were calculated using the nonparametric Kaplan-Meier method. The analysis accounts for data that needs to be censored as well as specialized non-normal distributions. The software generates a subsequent Wilcoxon score, to determine the statistical significance and test the homogeneity of the estimated survival function across the groups.

PCR

PCRs were run as follows: 1.5' 94° – [30" 94° – 30" annealing temperature – 30" 72°] x30 – 7' 72°. PCRs were used for verification of primer annealing temperatures prior to use in qPCR and qRT-PCR. Reactions were run according to lab

protocol. Reaction mixtures included 1.25 uL DNA, 1.25 uL 10x reaction buffer, 0.625 dNTPs, 0.5 uL of forward and reverse primers, 0.05 uL taq polymerase, and 2.08 uL ddH₂O. PCRs were run at a total volume of 6.25 uL for verification purposes, and large volume 25 uL when products would be used for subsequent experiments such as cloning or sequencing.

qPCR

qPCRs were performed at 60° annealing temperature unless otherwise indicated. 1X SYBR Green mix (Life Technologies) was used in along with the designated primers at a final concentration of 0.2 pmol/uL (Table 1). cDNA (100 ng) was diluted 1:16 in a 20 uL single reaction. Reactions were run in triplicate on a 96 well plate. A standard curve was generated for each primer set; dilutions were made at 1:4, 1:8, 1:16, 1:32, and 1:64. Standard curves used control (L4440) cDNA. This standard curve was then used to generate quantities in the experimental wells. qPCR experiments were run on both a PikoReal and ABI Real Time PCR machine. Degree of knockdown calculated using the following equation:

$$\frac{\frac{\text{Avg quantity (knockdown)}}{\text{Avg quantity (control)}}}{\frac{\text{Avg quantity (knockdown actin)}}{\text{Avg quantity (control actin)}}}$$

Creation of wCISD mutants

The new CRISPR/Cas 9 targeted genome editing system was used to create deletions in a targeted area of *wCISD*. A 20-nucleotide guide RNA sequence was cloned, using the Q5 site directed mutagenesis kit (NEB), into a 10ul reaction of PU6::*unc-119_sgRNA* vector (addgene). *Peft-3::cas9-SV40-NLS::tbb-2* 3'UTR (addgene) was used as the Cas9 vector with mCherry as an injection marker. Dr. Laura Mathies performed all injections into the gonad of N2 wild type worms. Following injections, worms recovered overnight and were subsequently picked onto individual 6cm NGM + OP50 plates. Progeny were scored; L1 larvae that fluoresced red were individually picked onto NGM + OP50 6 cm plates and allowed to grow developing potential knockout lines. An aliquot of these worms was taken for DNA extraction and subsequent sequencing.

RESULTS

Glucose Intolerance Lifespan Studies

Previous studies showed high glucose conditions in wild type (WT) nematodes reduced mean life span from 18.5 ± 0.4 to 16.5 ± 0.6 days and maximum life span from 25.9 ± 0.4 to 23.2 ± 0.4 days, independent of glucose effects on cuticle or bacterial metabolization of glucose (Schlotterer et. al. 2013). As the knockdown should lower the expression of the *wCISD2* gene, in the presence of high glucose concentrations, a significantly reduced lifespan was expected to be observed.

No successful lifespan analyses could be completed due to a high number of censors. Large numbers of animals became desiccated to the walls of the petri dish throughout ~17 trials over the course of 16 months. It was thought this was an attempt to avoid the change in osmolarity of the media secondary to the introduction of glucose. Initial glucose concentrations were taken from previous studies, (Schlotterer et. al. 2013), which had shown good outcomes. These studies, however, utilized N2 wild type and *eat-2* mutant animals. It is therefore probable that our CF3152 strain, which houses an *rrf-3* mutation, is more sensitive to the change in osmolarity.

Creation of wCISD mutants

CRISPR / Cas9 injected animals were individually picked to create potential knockout lines. Animals from the F₁ generation that fluoresced red (mCherry) were selected and transferred to fresh, individual, bacterially seeded plates. These animals were allowed to rest and reproduce for approximately 2-3 days. The F₁ offspring observed with fluorescence indicated the transgenic marker was transmitted. Fluorescent F₁ animals were again individually transferred onto new plates creating multiple distinct lines. These animals were subsequently allowed to reproduce for 2-3 days before their F₂ progeny were observed with the transgenic marker. Of the animals injected by Dr. Mathies, 10 F₁ lines were established. Of these 10 F₁ lines, 6 contained the observed mCherry co-injection marker. From there, a total of 3 transgenic F₂ lines were selected for transfer. Animals from all 3 lines were sent off for sequencing, none of which reported a mutation.

No recent confirmation of the WC-22 knockdown RNAi vector had been performed. Multiple qPCR trials were run between 2 separate real-time PCR machines (PikoReal and ABI). Primers were designed and approximately 20 qPCRs were run between the two. The tests showed varied C_T values between machines, but both presented the notion that the wCISD2 gene was over expressed in the animals by over a thousand. This was explained by a primer design error in which the qPCR

primers overlapped with the knockdown construct vector sequence. This registered a gross overexpression. New primers were redesigned to lie outside of the knockdown construct and a new qPCR assay was run in triplicate on the ABI machine. The results demonstrated no evidence of knockdown in the RNAi animal lines. All previous lifespan trials and experiments were voided, as the data was considered not reliable.

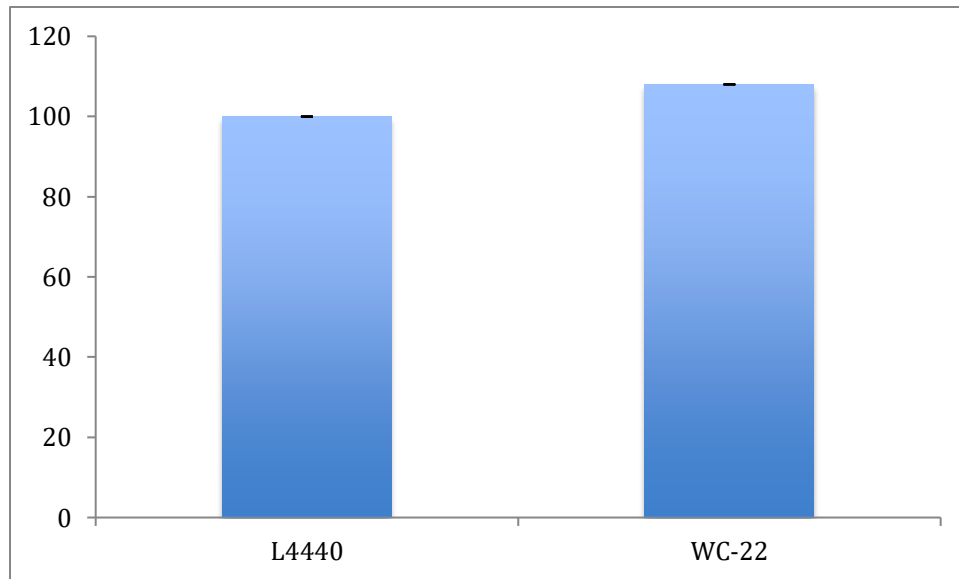


Figure 20: Confirmation of WC-22 knockdown

qRT-PCR analysis demonstrated an 8% overexpression in WC-22 expression and thus no knockdown was observed.

DISCUSSION

Subsequent to confirming an overexpression in the supposed wCISD knockdown animals the project came to a gradual halt. All previous trials and experiments were voided; data was not meaningful.

The CRISPR/Cas9 targeted genome editing system is used for site directed mutagenesis. The system uses a target sequence, which is specific to the gene of interest, to direct the Cas9 enzyme to the double stranded DNA (dsDNA), which induces subsequent cleavage. At this point, a higher likelihood of insertion or deletion (indel) mutation is possible secondary to non-homologous end joining DNA repair. This form of repair directly ligates the cleaved ends without the need for a homologous template. Amongst the recent advances and numerous promising CRISPR/Cas9 studies, however, the system is not without drawbacks. One caveat is that the indel may not cause a frame shift and thus fail to affect gene functionality. Furthermore, this system relies on a decreased efficiency of host repair mechanisms to spawn indels. Selection of transgenic animal lines is also not 100% efficient. The F₁ generation may contain many animals that appear transgenic, but these lines are not yet stable. In fact, a majority of the F₁ animals will not proliferate into stable F₂ lines.

Without identifying any wCISD mutant the project was temporarily terminated. A decision was made to resume studies on mitochondrial PNPase previously explored by former student Laura Lambert.

List of References

List of References

- Alodaib, Ahmad, Nara Sobreira, Wendy A. Gold et al. "Whole-exome sequencing identifies novel variants in *PNPT1* causing oxidative phosphorylation defects and severe multisystem disease." *European Journal of Human Genetics*, 25(2017): 79-84.
- Andrade, Jose M. and Cecilia M. Arraiano. "PNPase is a key player in the regulation of small RNAs that control the expression of outer membrane proteins." *RNA*, 14(2008): 543-551.
- Archer S (2013). Mitochondrial dynamics – mitochondrial fission and fusion in human diseases. *N Engl J Med* 369: 2236-2251.
- Balaban RS, Nemoto S, Tinkel T (2005). Mitochondria, oxidants, and aging. *Cell* 120(4): 483- 495.
- Bordone L and Guarente L (2005). Calorie restriction, SIRT1 and metabolism: understanding longevity. *Nat Rev Mol Cell Biol*. 6(4): 298-305.
- Brighton CT and Hunt RM (1974). Mitochondrial calcium and its role in calcification. *Clinical Orthopaedics and Related Research* 100(100): 406-416.
- Cao, Y., Meng, S., Chen, Y., Feng, J., Gu, D., Yu, B., . . . Gao, S. (2017). MFN1 structures reveal nucleotide-triggered dimerization critical for mitochondrial fusion. *Nature*, 542(7641), 372-376. doi:10.1038/nature21077
- Castandet B, Hotto AM, Fei Z, Stern DB (2013). Strand-specific RNA sequencing uncovers chloroplast ribonuclease functions. *FEBS Letters* 587(18): 3096-3101.
- Chen H, Chomyn A, Chan DC (2005). Disruption of fusion results in mitochondrial heterogeneity and dysfunction. *J Biol Chem* 280: 26185-26192
- Chen HW, Rainey RN, Balatoni CE, Dawson DW, Troke JJ, Wasiak S, Hong JS, McBride HM, Koehler CM, Teitell MA, French SW (2006). Mammalian polynucleotide homeostasis. *Mol Cell Biol*, 26(22), 8475–8487.
- Chial, H. & Craig, J. (2008) mtDNA and mitochondrial diseases. *Nature Education* 1(1):217

Corsi AK. A Biochemist's Guide to *C. elegans*. *Analytical biochemistry*. 2006;359(1):1-17. doi:10.1016/j.ab.2006.07.033.

Das SK, Sokhi UK, Bhutia S, Azab B, Su ZZ, Sarkar D, Fisher PB (2010). Human polynucleotide phosphorylase selectively and preferentially degrades microRNA-221 in human melanoma cells. *Proc Natl Acad Sci U S A*. 107(26): 11948–11953.

De Bono M (2003). Molecular approaches to aggregation behavior and social attachment. *J Neurobiol* 54(1):78-92

Dejean LM, Martinez-Caballero S, Kinnally KW (2006). Is MAC the knife that cuts cytochrome c from mitochondria during apoptosis? *Cell Death and Differentiation* 13(8): 1387-1395

Deng, Zhongliang, Zizhong Liu, Yjing Bi, Xiaoyi Yang, Dongsheng Zhou, Ruifu Yang and Yanping Han. "Rapid degradation of Hfq-free Ryhb in *Yersinia pestis* by PNPase independent of putative ribonucleolytic complexes." *BioMed Research International*, 2014 (2014): 1-7.

"Diabetes Mellitus." *Norml*. N.p., n.d. Web. 17 Oct. 2013.
<<http://norml.org/library/item/diabetes-mellitus>>.

Dillin A, Hsu AL, Arantes-Oliveira N, Lehrer-Graiwer J, Hsin H, Fraser AG, Kamath RS, Ahringer J, Kenyon C (2002). Rates of behavior and aging specified by mitochondrial function during development. *Science* 298(5602): 2398-2401.

Droge W (2002). Free radicals in the physiological control of cell function. *Physiol Rev*. 82(1): 47-95.

Favaro, Rebecca and Gianni Deho. "Polynucleotide Phosphorylase-Deficient Mutants of *Pseudomonas putida*." *Journal of Bacteriology*, 185.17(2003): 5279-5286.

Feng J, Frederic B, Hekimi S (2001). Mitochondrial electron transport is a key determinant of life span in *Caenorhabditis elegans*. *Dev Cell* 1(5): 633-644.

Fesik SW and Shi Y (2001). Controlling the Caspases. *Science*. 294: 1477-1478.

Friedland AE, Tzur YB, Esvelt KM, Colaiácovo MP, Church GM, Calarco JA. Heritable genome editing in *C. elegans* via a CRISPR-Cas9 system. *Nature methods*. 2013;10(8):741-743. doi:10.1038/nmeth.2532.

GeneCards. Weizmann Institute of Science, n.d. Web. 16 Oct. 2013. <<http://www.genecards.org/cgi-bin/carddisp.pl?gene=CISD2>>.

Genuth S, Alberti KG, Bennett P, Buse J, Defronzo R, Kahn R, Kitzmiller J, Knowler WC, Lebovitz H, Lernmark A, Nathan D, Palmer J, Rizza R, Saudek C, Shaw J, Steffes M, Stern M, Tuomilehto J, Zimmet P: Expert Committee on the Diagnosis and Classification of Diabetes Mellitus, the Expert Committee on the Diagnosis and Classification of Diabetes Mellitus. Follow-up report on the diagnosis of diabetes mellitus. *Diabetes Care* 2003; 26: 3160– 3167. 2003.

Germain A, Herlich S, Larom S, Kim SH, Schuster G, Stern DB (2011). Mutational analysis of Arabidopsis chloroplast polynucleotide phosphorylase reveals roles for both RNase PH core domains in polyadenylation, RNA 3'-end maturation and intron degradation. *The Plant Journal*. 67: 381-394.

Giannakou ME, Goss M, Junger MA, Hafen E, Leever SJ, Partridge L (2004). Long-lived *Drosophila* with overexpressed dFOXO in adult fat body. *Science* 305(5682): 361

Green DR (1998). Apoptotic pathways: the roads to ruin. *Cell* 94(6): 695-698

Gomes AF, Guimaraes EV, Carvalho L, Correa JR, Mendonca-Lima L, Barbosa HS (2011). *Toxoplasma gondii* down modulates cadherin expression in skeletal muscle cells inhibiting myogenesis. *BMC Microbiol*. 11: 110.

Haddad, Nabila, Odille Tresse, Katell Rivoal et al. "Polynucleotide phosphorylase has an impact on cell biology of *Campylobacter jejuni*." *Frontiers in Cellular and Infection Microbiology*, 2.30 (2012): 1-13.

Harris, T. (2016, April 13). Protein extraction from *C. elegans* using sea sand. Retrieved June 28, 2017, from <http://wbg.wormbook.org/2013/08/17/protein-extraction-from-c-elegans-using-sea-sand/>

Horvitz, H. R. (1997). A nematode as a model organism: the genetics of programmed death [Film]. Cogito Learning Media, Inc. Available: <http://www.cogitomedia.com> [1999, Jul 20]

Ishii N, Fujii M, Hartman PS, Tsuda M, Yasuda K, Senoo-Matsuda N, Yanase S, Ayusawa D, Suzuki K (1998). A mutation in succinate dehydrogenase cytochrome b causes oxidative stress and ageing in nematodes. *Nature* 394(6694): 694-697.

Kayser EB, Morgan PG, Hoppel CL, Sedensky MM (2001). Mitochondrial Expression and Function of GAS-1 in *Caenorhabditis elegans*. *J. Biol. Chem.*, 276: 20551–20558
Kenyon C, Chang J, Gensch E, Rudner A, Tabtiang R (1993). A *C. elegans* mutant that lives twice as long as wild type. *Nature* 366, 461–464

Kenyon C (2005). The plasticity of aging: insights from long-lived mutants. *Cell* 120, 449–460.

Kimura KD, Tissenbaum HA, Liu Y, Ruvkun G (1997). *daf-2*, an insulin receptor-like gene that regulates longevity and diapause in *Caenorhabditis elegans*. *Science* 277(5328): 942-946.

Lambert, L. (2015) *Phenotypic characterization of PNPase knockdown in C. elegans*. (Unpublished masters thesis). Virginia Commonwealth University, Richmond Virginia.

Lee SS, Lee RY, Fraser AG, Kamath RS, Ahringer J, Ruvkun G (2003). A systematic RNAi screen identifies a critical role for mitochondria in *C. elegans* longevity. *Nat Genet* 33: 40-48

Leszczyniecka M, DeSalle R, Kang DC, Fisher PB (2004). The origin of polynucleotide phosphorylase domains. *Mol Phylogenetics Evol* 31(1), 123–130.

Leszczyniecka M, Kang DC, Sarkar D, Su ZZ, Holmes M, Valerie K, Fisher PB (2002). Identification and cloning of human polynucleotide phosphorylase, hPNPase old-35, in the context of terminal differentiation and cellular senescence. *Proc Natl Acad Sci U S A.* 99(26): 16636–16641.

Leszczyniecka M, Su ZZ, Kang DC, Sarkar D, Fisher PB (2003). Expression regulation and genomic organization of human polynucleotide phosphorylase, hPNPase(old-35), a type I interferon inducible early response gene. *Gene*. 316, 143–156

Liu F, Gong J, Huang W, Wang Z, Wang M, Yang J, Wu C, Wu Z, Han B (2014). MicroRNA-106b-5p boosts glioma tumorigenesis by targeting multiple tumor suppressor genes. *Oncogene* 33(40): 4812-4822.

Liu X, Yu J, Jiang L, Wang A, Shi F, Ye H, Zhou X (2009). MicroRNA-222 regulates cell invasion by targeting matrix metalloproteinase 1 (MMP1) and manganese superoxide dismutase 2 (SOD2) in tongue squamous cell carcinoma cell lines. *Cancer Genomics Proteomics* 6(3): 131-139

Lupini L, Bassi C, Ferracin M, Bartonicek N, D'Abundo L, Zagatti B, Callegari E, Musa G, Moshiri F, Gramantieri L, Corrales FJ, Enright AJ, Sabbioni S, Negrini M (2013). miR-221 affects multiple cancer pathways by modulating the level of hundreds of messenger RNAs. *Front Genet* 4:64

M.A. Shakir and E.A. Lundquist. "Analysis of Cell Migration in *Caenorhabditis elegans*." *Methods Mol Biol*. 294: 159-74, 2004. PMID: PMC15576912.

Martinou JC and Youle RJ (2011). Mitochondria in apoptosis: Bcl-2 family members and mitochondrial dynamics. *Dev Cell*. 21(1): 92-101.

Miller RJ (1998). Mitochondria – the kraken wakes! *Trends in Neurosci* 21(3) 95-97.
Navarro A and Boveris A (2007). The mitochondrial energy transduction system and the aging process. *Am J Physiol Cell Physiol* 292(2): 670-686.

Mocellin, Simone, and Maurizio Provenzano. "RNA interference: learning gene knock-down from cell physiology." *Translational Medicine* 2 (2004): 39. Print.

Pardis S and Ruvkun G (1998). *Caenorhabditis elegans* Akt/PKB transduces insulin receptor-like signals from AGE-1 PI3 kinase to the DAF-16 transcription factor. *Genes Dev* 12(16): 2488-2498.

Piwowarski J, Grzechnik P, Dziembowski A, Dmochowska A, Minczuk M, Stepień P (2003). Human polynucleotide phosphorylase, hPNPase, is localized in mitochondria. *J Mol Biol*, 329(5), 853–857.

Raijmakers R, Egberts W, van Venrooij W, Pruijn GJM (2002). Protein-protein interactions between human exosome components support the assembly of RNase PH-type subunits into a six-membered PNPase-like ring. *J Mol Biol.* 323(4): 653–663

Rainey R, Glavin J, Chen H, French S, Teitell M, Koehler C (2006). A new function in translocation for the mitochondrial i-AAA protease Yme1: Import of polynucleotide phosphorylase into the intermembrane space. *Mol Cell Biol.* 26(22): 8488–8497.

Rambold AS, Kostelecky B, Elia N, Lippincott-Schwartz J (2011). Tubular network formation protects mitochondria from autophagosomal degradation during nutrient starvation. *Proc Natl Acad Sci U S A* 108(25): 10190-10195.

Rankin CH (2002). From gene to identified neuron to behavior in *Caenorhabditis elegans*. *Nat Rev Genet.* 3(8): 622-630

Regonesi, Maria Elena, Federica Briani, Andrea Ghetta et al. “A mutation in polynucleotide phosphorylase from *Escherichia coli* impairing RNA binding and degradosome stability.” *Nucleic Acid Research*, 32.3 (2004): 1006-1017.

Rigoli, L., & Bella, C. D. (2012). Wolfram syndrome 1 and Wolfram syndrome 2. *Current Opinion in Pediatrics*, . doi:10.1097/mop.0b013e328354ccdf

Rizzuto R, Marchi S, Bonora M, Aguiari P, Bononi A, De Stefani D, Giorgi C, Leo S, Rimessi A (2009). Ca²⁺ transfer from the ER to mitochondria: when, how, and why. *Biochem Biophys Acta* 1787(11): 1342-1351.

Robb EL, Christoff CA, Maddalena LA, Stuart JA (2013). Mitochondrial reactive oxygen species (ROS) in animal cells: relevance to aging and normal physiology. *Can J Zoo* 92(7): 603- 613

Rodriguez M, Snoek LB, De Bono M, Kammenga JE (2013). Worms under stress: *C. elegans* stress response and its relevance to complex human disease and aging. *Trends Genet.* 29(6): 367-374.

Sarkar D and Fisher PB (2006). Human polynucleotide phosphorylase (hPNPase old-35): An RNA degradation enzyme with pleiotrophic biological effects. *Cell Cycle* 5(10): 1080–1084.

Sarkar D and Fisher PB (2006). Molecular mechanisms of aging-associated inflammation. *Can Let.* 236(1): 13–23.

Sarkar D and Fisher PB (2006). Polynucleotide phosphorylase: An evolutionary conserved gene with an expanding repertoire of functions. *Pharm Therap* 112(1): 243–263.

Sarkar D, Lebedeva IV, Emdad L, Kang DC, Baldwin AS, Fisher PB (2004). Human polynucleotide phosphorylase (hPNPaseold-35): A potential link between aging and inflammation. *Can Res* 64(20): 7473–7478.

Sarkar D, Park ES, Fisher PB (2006). Defining the mechanism by which IFN β downregulates c-myc expression in human melanoma cells: Pivotal role for human polynucleotide phosphorylase (hPNPaseold-35). *Cell Death Diff* 13(9): 1541–1553

Sarkar D, Leszczyniecka M, Kang DC, Lebedeva I, Valerie K, Dhar S, Pandita TK, Fisher PB (2003). Downregulation of Myc as a potential target for growth arrest induced by human polynucleotide phosphorylase (hPNPaseold-35) in human melanoma cells. *J Biol Chem* 278:24542–51

Sarkar D, Park ES, Emdad L, Randolph A, Valerie K, Fisher PB (2005). Defining the domains of human polynucleotide phosphorylase (hPNPaseold-35) mediating cellular senescence. *Mol Cell Biol* 25: 7333-7343.

Sarkar D, Park ES, Barber GN, Fisher PB (2007). Activation of double-stranded RNA-dependent protein kinase, a new pathway by which human polynucleotide phosphorylase (hPNPaseold-35) induces apoptosis. *Cancer Res* 67(17): 7948-7953

Schaffitzel E and Hertweck M (2006). Recent aging research in *Caenorhabditis elegans*. *Exp Gerontol* 41(6): 557-563.

Schlotterer, Andreas et. al "Diabetes." *C. elegans as Model for the Study of High Glucose– Mediated Life Span Reduction*. Version vol. 58. N.p., n.d. Web. 5 Sept. 2013.<<http://diabetes.diabetesjournals.org/content/58/11/2450.full>>.

Schulz TJ, Zarse K, Voigt A, Urban N, Birringer M, Ristow M (2007). Glucose restriction extends *Caenorhabditis elegans* life span by inducing mitochondrial respiration and increasing oxidative stress. *Cell Met* 6(4): 280-293.

Sena LA and Chandel NS (2012). Physiological roles of mitochondrial reactive oxygen species. *Mol Cell* 48(2): 158-167.

Shigenaga MK, Hagen TM, Ames BN (1994). Oxidative damage and mitochondrial decay in aging. *Proc. Natl. Acad. Sci. USA* 91: 10771-10778

Sokhi UK, Das SK, Dasgupta S, Emdad L, Shiang R, DeSalle R, Sarker D, Fisher PB (2013). Human polynucleotide phosphorylase (*hPNPase^{old-35}*): should I eat you or not – that is the question? *Adv Can Res* 119: 161-190.

Sokhi UK, Manny D, Bacolod, Luni Emdad, et al. "Analysis of global changes in gene expression induced by human polynucleotide phosphorylase (*hPNPase^{old-35}*)." *Cell Physiology*, 229.12(1952-1962.)

Shore DE, Carr CE, Ruvkun G (2012). Induction of Cytoprotective Pathways Is Central to the Extension of Lifespan Conferred by Multiple Longevity Pathways. *PLoS Genet* 8(7): e1002792.

Sönnichsen B, Koski LB, Walsh A, Marschall P, Neumann B, Brehm M, Alleaume AM, Artelt J, Bettencourt P, Cassin E, Hewitson M, Holz C, Khan M, Lazik S, Martin C, Nitzsche B, Ruer M, Stamford J, Winzi M, Heinkel R, Röder M, Finell J, Häntsch H, Jones SJ, Jones M, Piano F, Gunsalus KC, Oegema K, Gönczy P, Coulson A, Hyman AA, Echeverri CJ (2005). Full-genome RNAi profiling of early embryogenesis in *Caenorhabditis elegans*. *Nature* 434(7032): 462-469.

Stickney L, Hankins J, Miao X, Mackie G (2005). Function of the conserved S1 and KH domains in polynucleotide phosphorylase. *J Bact* 187(21): 7214–7221

Stiernagle, Theresa. "Maintenance of *C. elegans**." *Maintenance of C. elegans*. Worm Book, n.d. Web. 17 Oct. 2013.
<http://www.wormbook.org/chapters/www_strainmaintain/strainmaintain.html>.

Van Raamsdonk JM and Hekimi S (2012). Superoxide dismutase is dispensable for normal animal lifespan. *Proc natl Acad Sci U S A*. 109(15): 5785-5790.

Vedrenne V, Gowher A, De Lonlay P, Nitschke P, Serre V, Boddaert N, Altuzarra C, Mager- Heckel AM, Chretien F, Entelis N, Munnich A, Tarassov I, Rotig A (2012). Mutation in PNPT1, which encodes a polyribonucleotide nucleotidyltransferase, impairs RNA import into mitochondria and causes respiratory-chain deficiency. *Am J hum Genet* 91(5): 912-918.

Viegas, Sandra C, Verena Pfeiffer, Alexandra Sittka et al. "Characterization of the role of ribonucleases in *Salmonella* small RNA decay." *Nucleic Acid Research*, 35.22(2007): 7651-7664.

Von Ameln S, Wang G, Boulouiz R, Rutherford MA, Smith GM, Li Y, Pogoda HM, Nurnberg G, Stiller B, Volk AE, Borck G, Hong JS, Goodyear RJ, Abidi O, Nurnberg P, Hofmann K, Richardson GP, Hammerschmidt M, Moser T, Wollnik B, Koehler CM, Teitell MA, Barakat A, Kubish C (2012). A mutation in PNPT1, encoding mitochondrial-RNA-import PNPase, causes hereditary hearing loss. *Am J Hum Genet* 91(5): 919-927.

Walker G, Houthoofd K, Vanfleteren JR, Gems D (2005). Dietary restriction in *C. elegans*: from rate-of-living effects to nutrient sensing pathways. *Mech. Ageing Dev.* 126: 929–937

Wang G, Chen H, Oktay Y, Zhang J, Allen E, Smith G, Fan KC, Hong JS, French SW, McCaffery JM, Lightowlers RN, Morse HC, Koehler CM, Teitell MA (2010). PNPASE regulates RNA import into mitochondria. *Cell* 142(3): 456–467.

Wang G, Shimada E, Koehler C, Teitell M (2012). PNPASE and RNA trafficking into mitochondria. *Bioch Biophys Acta* 1819(9–10): 998–1007.

Weinberg F and Chandel NS (2009). Mitochondrial metabolism and cancer. *Annals of NY Acad Sci.* 1177: 66-73.

Wong A, Boutis P, Hekimi S (1995). Mutations in the *clk-1* gene of *Caenorhabditis elegans* affect development and behavioral timing. *Genetics* 139: 1247–1259

"WormClassroom." *A Short History of C. elegans Research*. University of Wisconsin-Madison, n.d. Web. 2 Oct. 2013. <<http://wormclassroom.org/short-history-c-elegans-research>>.

Wu, Jinhua and Li Zhongwei. "Human polynucleotide phosphorylase reduces oxidative RNA damage and protects HeLa cell against oxidative stress. *Biochemistry and Biophysics Research Communications*, 372.2 (2008): 288-292.

VITA

Danielle Keary Seibert was born April 24, 1990, in Cook County Illinois. She graduated from Neuqua Valley High School, Naperville, Illinois in 2008. She received her Bachelor of Science in Cellular and Molecular Biology, with honors, from Limestone College, Gaffney, South Carolina in 2012 at which time she worked in the Illinois State Crime Lab.